Preliminary Fracture Mechanics Analysis of Cleaning Equipment in Hydrogen Mixture Service

Prepared for:	National Gas Transmission
Doc Ref:	811356-00-PR-REP-0001
Rev:	02
Date:	April 2026

Report

wood.

Client	
National Gas Transmission	
Preliminary Fracture Mechanics Analysis of Cleaning Equipment in Hydrogen Mixture Service	
811356-00-PR-REP-0001	TBC

Stephen Mathews, Principal Process Engineer
Stephen.Mathews@woodplc.com

Wood
Sir Ian Wood House
Hareness Road
Altens Industrial Estate
Aberdeen AB12 3LE
Scotland, UK

Tel +44 (0)1224 851000
www.woodplc.com

Revision	Date	Reason for Issue	Prepared	Checked	Approved
			Harry Cotton Digitally signed by Harry Cotton Date: 2026.04.23 16:56:09 +01'00'	Yuri Tkach 2026.04.23 17:38:03 +01'00'	stephen mathews
02	24/04/2026	Issued for Use	HC	YT	SM
01	11/03/2026	For Review	YT	HC	SM

Revision History (Optional)		
Revision	**Date**	**Comments**
01	11/03/26	For Review
02	24/04/26	Issued for Use

HOLDS		
No.	**Section**	**Comment**

Signatory Legend		
Revision	**Role**	**Comments**
02	Prepared	Yuri Tkach
	Checked	Harry Cotton
	Approved	Stephen Mathews

1.0 Executive Summary

National Gas Transmission (NGT) is investigating the capabilities of their network for a pure hydrogen or blended gas service. This study is part of a broader initiative to support the UK's Net Zero targets by enabling the transition of the National Transmission System (NTS) to accommodate hydrogen, either as a blend or in pure form. Previous studies by Wood for NGT [7,8] indicate that hydrogen levels as low as 1 % will significantly reduce the cracking resistance (i.e. cause embrittlement) of the carbon steel from which the pipelines and associated equipment are constructed.

The cracking resistance of the carbon steel pipelines of NTS, after conversion to hydrogen/mixture service, is being evaluated by NGT using a fracture mechanics (FM) approach [10]. This is a calculation procedure predicting the critical limits for the key parameters which govern the stability or propagation of crack-like (planar) flaws as follows:

- Stress level (tensile and cyclic):
- Flaw size. (Existing crack-like flaws accepted in inspection in fabrication/welding):
- Material cracking resistance determined by destructive tests in hydrogen pressure environment.

If two of the above parameters are known a limit for the third can be predicted to avoid propagation of flaws in the pipeline in hydrogen/mixture service.

The NTS also includes various equipment for cleaning the gas including scrubbers (separators) which are carbon steel pressure vessels fabricated by welding. This report describes a study to investigate if the fracture mechanics (FM) approach can prove the cracking resistance of typical scrubbers converted to 20% hydrogen and 100% hydrogen service.

[redacted]

The FM analysis was conducted following approaches in BS 7910 [17]. The scrubbers were assumed to be subjected to the tensile stresses predicted, using an analytical equation, under the maximum design pressure. Finite element analysis (FEA) was used to determine the stress levels in the complex stress field around the manway nozzle.

The FM analysis took account of tensile residual stresses in the welds following BS 7910 [17]. The residual stresses in welds of the main upper vessel were assumed to be relieved beneficially to low levels by the post weld heat treatment (PWHT) conducted in fabrication. However, the residual stress in the lower vessel (boot) was assumed to be much higher since it was not subjected to PWHT.

The cyclic stress acting on the vessels was estimated from operating pressure cycles recorded in the NTS at a site adjacent to the scrubber assuming 50 years in converted service. The analysis also assessed the hypothetical scenario that the scrubber is subjected to additional pressure cycles due to complete depressurisations (shut down) for maintenance or repair once each year.

The assumed level of steel cracking resistance under static stress (i.e. toughness) was estimated from results of FM tests conducted on linepipe and weld samples in a hydrogen pressure chambers. A toughness ($K_{mat,H}$) value of 55 $\mathrm{MPa}\sqrt{\mathrm{m}}$ was assumed as base case which is typically achievable in testing carbon steel linepipe and welds.

Further sensitivity study covered a toughness range (40MPa$\sqrt{m}$ to 75 MPa$\sqrt{m}$) determined in a program of testing various linepipes and welds [15] under 220 bara hydrogen pressure.

The scrubber was assumed to contain weld flaws up to the maximum sizes accepted in inspection of the welds by ultrasonic testing (UT) in vessel fabrication/welding.

The effect of hydrogen in accelerating fatigue crack growth of weld defects under the cyclic stresses was accounted for using a published fatigue crack growth law by Sandia National Laboratories [18]. It is based on results of fatigue crack growth tests conducted on carbon steel samples under hydrogen pressure.

The FM analysis indicated that the main upper vessel is resistant to cracking in hydrogen mixture service including main seam welds and nozzle welds. The internal crotch corner of the manway nozzle was predicted to be crack sensitive due to high stress concentration (Figure 5-7). However, this area is unwelded parent material so would not be expected to contain pre-existing crack-like (planar) flaws to propagate.

The smaller lower vessel (boot) was predicted to be crack resistant under maximum design pressure and operating pressure cycles though the margins of acceptability are small, compared to the upper vessel, since it was not subjected to relief of residual stresses by PWHT in fabrication.

In order to confirm acceptability for hydrogen mixture conversion the scrubbers should be subjected to inspection by phased array ultrasonic methods. This may be conducted opportunistically to coincide with routine inspections.

The assumed toughness level in the FM analysis should be further confirmed by tests on samples of representative pressure vessel steel and welds in hydrogen. This is subject to samples being obtainable possibly from redundant NGT scrubbers. The degree of necessity for this testing depends on the results of the phased array UT examination and the size of any flaws detected which need to be justified.

Based on the above, the FM analysis demonstrates that the scrubbers can be proven to be crack resistant in future hydrogen /mixture service by such approach. This is subject to confirmation that the assumptions are conservative by further NDT, stress analysis and also material testing in hydrogen if necessary, conducted on redundant scrubbers, as explained above. It is expected that this further work will confirm cracking resistance for the upper vessel and probably also for the lower vessel though the outcome is less certain.

[redacted] scrubber conical head area is an exception since it is subjected to much higher stress than the other scrubbers. Further survey of the scrubbers at other NGT sites, which are candidate for hydrogen/mixture conversion, should be made to clarify their key characteristics and determine the extent of further FM analysis needed to assess suitability for conversion.

The cost of FM analysis, associated stress analysis, material testing in hydrogen and NDT should be estimated and compared with the alternative option of replacement with new scrubbers which confirm with ASME code [32] requirements for vessels in hydrogen service.

Table of Contents

[redacted]

TABLES

2.0 INTRODUCTION

2.1 Project Overview – Impact of Hydrogen on Gas cleaning assets

The conversion of the NTS into a blended hydrogen transmission network involves several challenges and extensive work is underway to prove the technical capability and commercial viability of converting the existing network to a blended hydrogen network. In parallel, Project Union is underway to provide a 100% hydrogen core network for the UK allowing the major production sites and industrial clusters to be linked.

The NTS has a numerous separators, filters and strainers that have been grouped as "gas cleaning assets" for the purpose of this project. It has been identified that the other NIA funded projects are not investigating hydrogen impact on these assets in any significant detail.

2.2 Network overview

National Gas Transmission owns and operates Britain's National Transmission System (NTS) for gas. This complex matrix of pipelines transports gas from its points of entry to power stations, industrial plants, storage facilities and to the local Gas Distribution Networks that take gas into homes and businesses, as well as overseas via interconnectors. The NTS comprises around 5,000 miles of pipeline, more than 60 compressors at 21 compressor stations and more than 500 above-ground installations (AGI).

At the various AGIs and compressor stations, the gas may have liquid or solid contaminants that should be removed. This is achieved by scrubbers and filters respectively.

2.3 Background

The introduction of hydrogen into the NTS will reduce the cracking resistance (i.e. cause embrittlement) of the carbon steel from which the pipelines and associated assets are constructed.

The cracking resistance of the carbon steel pipelines of NTS after conversion to hydrogen/mixture service is being evaluated by NGT using a fracture mechanics (FM) approach [10]. This is a calculation procedure predicting the critical limits for the key parameters which govern the stability or propagation of crack-like flaws (stress, flaw size, material properties in hydrogen)

A previous study for NGT [9] assessed the suitability of the materials of construction of existing gas cleaning equipment for service in hydrogen mixture service. It was established that the separators/scrubbers are pressure vessels fabricated from carbon steel which would undergo a reduction in cracking resistance (i.e. embrittlement) due to the effects of hydrogen gas. It was recommended that further investigation be conducted to assess if the FM approach, being applied to the pipelines [10], could also be used to confirm cracking resistance of scrubbers in hydrogen mixture service.

2.4 Document Purpose and Work

This report presents a trial FM analysis of an example scrubber (i.e. separator) to assess the likelihood of being able to confirm equipment cracking resistance and integrity by such an approach.

Other equipment such as filters and pig launcher/receiver are excluded from this study.

2.5 Abbreviations

Abbreviation	Definition
AGI	Above-Ground Installations
API	American Petroleum Institute
ASME	American Society of Mechanical Engineers
ASTM	American Society for Testing and Materials
BS	British Standard
CTOD	Crack Tip Opening Displacement
DAC	Distance Amplitude Curve
DNV	Det Norske Veritas
da/dN	Crack growth rate
EPRG	European Pipeline Research Group
FAD	Failure Assessment Diagram
FCG	Fatigue Crack Growth
FM	Fracture Mechanics
H2PIPE	DNV Joint Industry project in hydrogen pipelines
HHV	Higher Heating Values
JIP	Joint Industry Project
K	Stress Intensity Factor
$K_{mat,H}$	Fracture toughness in terms of critical stress intensity in hydrogen [35].
$K_{mat,H,th}$	Fracture toughness in hydrogen measured at the initiation of crack growth in rising displacement test [35].
$K_{0.05mm}$	Stress intensity at 0.05 mm of crack extension as measured in rising displacement test [35]
$K_{max\ load}$	Stress intensity at maximum load as measured in rising displacement test.
LoF	Lack of Fusion

LoP	Lack of Penetration
MPI	Magnetic Particle Inspection
NDT	Non-Destructive Testing
NG	Natural Gas
NGT	National Gas Transmission
NTS	National Transmission System
OD	Outside Diameter
PWHT	Post Weld Heat Treatment
SCF	Stress Concentration Factor
UT	Ultrasonic Testing
WT	Wall Thickness

3.0 DESIGN DATA

3.1 Introduction

Detailed information for the scrubbers (Separators) located at [redacted] sites was obtained in the form of fabricators drawings [1,2,3]. These show dimensions, material grades and design parameters. Extracts from the scrubber drawings are shown Appendix A.

[redacted] (1250 mm, 2750 mm, 1519 mm diameter) [redacted] (712 mm, 915 mm, 915 mm diameter) [redacted] but the lower vessels are as-welded since it is not mandatory [4] for thickness ≤40 mm.

The scrubber shells are made from normalised weldable carbon steel pressure vessel steels of similar specification and grade in accordance with BS 1501 Part 1[5] or its successor BS EN 10028.

[redacted] [3] was not selected since it is unlikely to be converted to hydrogen mixture service.

The Table 3-1 indicates the maximum design stress (hoop stress) at maximum design pressure. The Avonbridge [redacted] (44 mm thickness) [redacted]

The findings of this assessment cover three scrubbers of identical design [1] manufactured [redacted] e and are indicative for the other scrubbers since they are of similar design and steel specification but it is necessary to take account of the high stress in [redacted] as explained above (Table 3-1).

Some information for scrubbers [redacted] was also obtained but was not sufficient to conduct analysis with detailed fabricator drawings not yet located. Further surveys of the scrubbers at all other NGT sites, which are candidate for hydrogen/mixture conversion, is required to clarify their key characteristics (design, dimensions, stress levels, steel grades, PWHT extent) and clarify the applicability of the findings of this study to them.

[redacted]

National Gas Site	Manufacturer	Date of Design/Manufacture	Number of Scrubber/Separator manufactured	Design Pressure, barg	Design Temperature, °C	Component	Dimensions		Hoop Stress, MPa (Note 1)	Stress Utilization % (hoop stress/SMYS)	Shell Steel Grade	Specified Minimum Yield Strength (SMYS), MPa	UTS, MPa
							Diameter, mm	Thickness, mm					
[redacted]	Glapwell	2005	3	[redacted]	[redacted]	Shell (cylinder)	[redacted]	[redacted]	[redacted]	[redacted]	BS 1501-224-490B LT50	[redacted]	[redacted]
						Heads (cone)		[redacted]	[redacted]	[redacted]	BS 1501-224-490B LT50	[redacted]	[redacted]
[redacted]	Peerless	2003	2	[redacted]	[redacted]	Shell (cylinder)	[redacted]	[redacted]	[redacted]	[redacted]	BS EN 10028-355-NH	[redacted]	[redacted]
						Head (cone)		[redacted]	[redacted]	[redacted]	BS EN 10028-355-NH		
[redacted]	Wefco	2018	2	[redacted]	[redacted]	Shell (cylinder)	[redacted]	[redacted]	[redacted]	[redacted]	BS EN 10028-355-NH &NL1	[redacted]	[redacted]
						Head (dished end)		[redacted]	[redacted]	[redacted]	BS EN 10028-355-NH &NL2		

Note 1: Hoop stress calculated at maximum design pressure using equation 1 Section 3.

3.2 Assumptions

3.2.1 General

The [redacted] selected for analysis is shown in Fig 3.1 below [1] which indicates the welds joints selected (Joints 1 to 5) for FM analysis (Section 3.3 below).

The material properties, dimensions and geometry assumed in assessment of the [redacted] are covered below.

[redacted]

3.2.2 Material Properties

3.2.2.1 Tensile Strength Properties

The published research indicates that tensile strength properties are not affected significantly by hydrogen gas.

The vessel main shell was fabricated from steel plates conforming to BS 1501[5], steel type 224 and grade 490.

The steel is fully killed carbon manganese steel heat treated by normalising.

The nozzle was specified as ASTM A333 Grade 8 [6] which is carbon steel pipe.

The minimum specified tensile properties assumed are summarised in **Table 3-2** below including specified minimum yield strength (SMYS) and minimum ultimate tensile strength (UTS). Mill certificates were not available for the steel to clarify actual measured tensile properties.

Table 3-2 Summary of [redacted] Scrubber steel grades and specified minimum tensile properties assumed [1].

Area	Location	Steel Grade	SMYS, MPa	UTS, MPa	Internal Diameter, mm	Thickness, mm
[redacted]	[redacted]	[redacted]	[redacted]	[redacted]	[redacted]	[redacted]
[redacted]	[redacted]	[redacted]	[redacted]	[redacted]	[redacted]	[redacted]
[redacted]	[redacted]	[redacted]	[redacted]	[redacted]	[redacted]	[redacted]
[redacted]	[redacted]	[redacted]	[redacted]	[redacted]	[redacted]	[redacted]

3.2.2.2 Toughness

This section justifies the assumed toughness levels, in the hydrogen pressure service, for the FM analysis based on existing toughness test data prior to testing of representative scrubber steel and welds in hydrogen. The toughness is the material resistance to crack propagation of existing flaws under static maximum tensile stress. The effect of hydrogen on crack propagation under cyclic stress (fatigue) is accounted for using a published fatigue crack growth law as explained in Section 4.

The toughness in hydrogen is measured using pre-cracked specimens subjected to load (displacement) in hydrogen pressure chambers. The extensive published test data reviewed in the previous study for NGT [7,8] indicates that the toughness of carbon steels is reduced substantially by the effects of hydrogen gas.

The potential effect of hydrogen on the toughness of the steels of cleaning equipment was reviewed in the previous study for NGT [9] considering data available for carbon steel pipeline steels and comparing their metallurgy with those of the scrubbers. No relevant published results of toughness tests in hydrogen on carbon steel pressure vessel steels were found. Sandia National Laboratories have published results [18] of toughness tests on pressure vessel steels but they were low alloy steels of much higher strength than the scrubber carbon steel grades and the test methods may not comply fully with the latest recommendations.

The expected toughness may be judged from results of tests on carbon steel linepipe and welds in hydrogen. The pipeline industry has adopted testing methods using rising displacement, based on elastic plastic fracture mechanics (EPFM), which have undergone development over recent years in terms of control of test parameters, hydrogen environment purity and interpretation of results. Much of the published test data does not comply with the latest detailed testing methods [11] and is potentially non-conservative. Therefore, the toughness assumptions are judged against the results of a program of tests conducted by DNV for NGT [8,12,13], on Grade API 5L X60

1970's linepipe (415 MPa SMYS) from NTS, using the latest developed testing methods. The effect of hydrogen partial pressure on toughness, corresponding to hydrogen blended into the system, is summarised in Table 3-3 below. The results suggest that a toughness ($K_{mat,H}$) exceeding 77 $MPa\sqrt{m}$,corresponding to $K_{0.05mm}$, may be achieved with 20% hydrogen (18 bara H_2) reducing to 63 $MPa\sqrt{m}$ at 100% hydrogen (91 bara Hydrogen).

However, considering the possible differences in metallurgy, between the carbon steel pipe tested and the scrubber carbon steel vessel steels and welds described in previous study [9], a toughness of 55 $MPa\sqrt{m}$ was assumed as base case. The value of 55 $MPa\sqrt{m}$ is also the minimum allowed according to ASME B31.12 [14] for FM testing pipeline steels in hydrogen though the specified test method is no longer regarded as reliable.

Further sensitivity study was made assuming a toughness ($K_{mat,H}$) minimum of 40 $MPa\sqrt{m}$ and maximum of 75 $MPa\sqrt{m}$. This is about the range recorded, in terms of both $K_{mat,H,th}$ and corresponding to $K_{0.05mm}$, as part of the H2PIPE joint industry project [15] and using the latest testing methods [11]. A variety of linepipe metallurgies were tested, including some weld metal and heat affected zone (HAZ), at hydrogen pressures of 210 barg which far exceeds the rating of the NTS.

Based on the above (Ref 11), there is confidence that a toughness level ($K_{mat,H}$) of 40 $MPa\sqrt{m}$ is conservative for the weldable carbon steels of the scrubbers. However, the toughness assumptions should be confirmed by testing samples of representative pressure vessel steel and welds in hydrogen which may be obtainable from redundant NGT scrubbers.

The results of toughness tests conducted by NGT on an extensive range of samples of linepipe and welds from NTS [34], under 69 bara hydrogen pressure, should also be considered to further clarify conservatism of toughness assumptions.

Table 3-3 Results of Toughness Tests in hydrogen conducted on NGT X60 (415 MPa SMYS) linepipe from NTS [8,12,13] .

Hydrogen % (Assuming 90 barg)	**Hydrogen partial pressure bara**	$K_{mat,H,th}$ $MPa\sqrt{m}$	$K_{0.05mm}$ ***(Note 3)*** $MPa\sqrt{m}$
0.0	0	117	126 (Note 2)
0.6	0.5	65	99
1.1	1	61	78
3.9	3.5	54	77
15.6	14	54	80
20.0 (Note 1)	18	53	**77**
38.9	35	50	65
77.8	70	47	**63**
>100.0	100	45	67

Note 1: Interpolated result.

Note 2: 172 $MPa\sqrt{m}$ recorded in air in terms of $K_{max\ load}$

Note 3: The acceptance of toughness corresponding to $K_{0.05mm}$ as a valid assumption is subject to confirmatory constant load testing to prove crack stability according to DNV-RP-F123[35].

3.2.3 Flaw Assumptions Defect Sizes

The FM analysis assumed planar (crack-like) flaws in the welds which are accepted in non-destructive testing (NDT) in vessel fabrication welding.

The scrubber full penetration welds were subjected to 100% NDT by radiography and ultrasonic testing (UT) (Ref 1) as required by PD5500 [4] in fabrication. The assumed maximum size of planar (crack like) flaws was based on the NDT acceptance criteria [1,4].

The radiographic acceptance criteria (PD 5500, Table 5.7-1) do not permit cracks or planar flaws such as lack of fusion or penetration. However, this inspection method does not reliably detect such flaws depending on their orientation relative to the X-ray beam.

The UT acceptance criteria (PD 5500, Table 5.7-2) state the allowable length of planar flaws, parallel to the weld (longitudinal), depending on the ultrasonic echo response height as a percentage of the distance amplitude curve (DAC) height. The DAC defines ultrasonic response height in a calibration by ultrasonic scanning a steel block with machined side drilled holes of 3 mm diameter.

The maximum allowable length (PD 5500, Table 5.7-2) ranges from 5 mm (50% to 100% DAC echo height) to a length of half thickness (20% to 50% DAC echo height). Furthermore, surface breaking flaws are restricted to 5 mm length (20% to 100% DAC echo height). To be conservative, the maximum allowable length, applicable for the lowest echo height (20% to 50% DAC) was assumed which is a length equal to half thickness.

The manual UT does not reliably determine flaw height. Nevertheless, planar flaws such as lack of fusion or penetration, in multi-pass arc welds, are normally confined within a single weld pass (run) which rarely exceed 3 mm height. Therefore, the effective flaw maximum flaw height of the UT acceptance criteria was assumed to be 3 mm. It should be noted that this approach is fundamental to radiographic acceptance criteria in which flaw height is not measured.

Based on the above, the FM analysis assumed the below maximum flaw sizes in the scrubber full penetration welds.

Table 3-4 Flaw sizes assumed present in welds (UT acceptance criteria)

Weld Joint (Figure 3-1)	Thickness, mm	Flaw Height, mm	Flaw Length, mm
4	50	3	25
1	40	3	20
2 & 3	35	3	17.5
5	20	3	10

In the main seams flaws are assumed to be orientated parallel to the welds and perpendicular to the plate surface. The flaw orientation at the manway nozzle weld is covered in Section 4.

Reports of NDT in fabrication were not available but would most likely just confirm welds as meeting acceptance criteria and not report actual flaw sizes. Further inspection using advanced methods, such phased array UT techniques, would be required to confirm the actual size of welding/fabrication flaws in the scrubber.

The scrubbers clean processed dry gas which is not expected to contain significant levels corrosive contaminants (H_2O, O_2, CO_2, H_2S), so internal corrosion damage (metal loss, corrosion cracking) is not expected, and external corrosion should be preventable by coating. The scrubber is not expected to contain fatigue cracks from previous natural gas service since the level of pressure cycling anticipated is benign and much less severe than assumed in design (See Section 3.3.4).

A report of in-service inspection [16], conducted in 2024, gives results of ultrasonic testing (UT) to check wall thickness which confirmed no significant corrosion damage. An internal surface inspection by magnetic particle inspection (MPI) was also reported indicating no in-service crack-like indications. Sharp toe inter-run indications were reported which are much smaller than the flaw sizes assumed (Table **3**-**4**) so effectively assessed conservatively in the FM analysis.

3.3 Applied Stresses

3.3.1 General

The analysis covered longitudinal and circumferential seam (girth) welds in the main (upper) vessel (joints 1,2 and 3 Figure 3-1) and lower vessel (Joint 5 Figure 3-1) .

Finite element analysis (FEA) of the manway nozzle (Joint 4, Figure 3-1) was conducted to estimate the stress concentrating effects as explained in Section 5.1. The manway (Joint 4, Figure 3-1) is by far the largest opening (nozzle) in the main (upper) vessel shell (Fig 1) so is expected to cause the most severe stress concentrating effect. This should be confirmed in further work to assess the stress concentrating effect at the small diameter (2 inch OD) set on nozzles (e.g. joint 6, Figure 3-1) and nozzle connecting the lower vessel to the upper vessel (joint 7, Figure 3-1).

The analysis also took account of the stress concentrating effects at welds, due to weld geometry/profile, misalignment at the joints and transitions in thickness or diameter, using the equations of BS 7910 [49] as explained in Section 4 below.

The tensile residual stresses in welds, due to thermal contraction after welding, were also taken into account using the equations of BS 7910 [17] as explained in Section 3.3.3 below.

3.3.2 Peak Primary Stresses

3.3.2.1 General

The maximum applied tensile nominal stresses were calculated from design pressure levels using the below equation by Barlow:

$$\sigma = \frac{PD}{2T} \qquad ......(1)$$

σ = Stress perpendicular to vessel axis (i.e. hoop stress). Stress transverse to vessel axis equals $\sigma/2$.
P = Maximum design pressure
D = Median diameter
T = Thickness

The tensile stresses, under the maximum design pressure (90 barg), predicted using equation 1, are presented in Table **3**-**5** below.

Table 3-5 Maximum nominal tensile stresses, transverse to welds, in [redacted] Scrubber at maximum design pressure of 90 barg. Determined by equation 1 above.

Location	Joint number (Figure 3-1)	Seam orientation	Internal Diameter, mm	Thickness, mm	Hoop stress, MPa (Note1)

[redacted]

Note 1: Hoop stress transverse to vessel or nozzle axis as applicable.

The scrubber was hydrotested (proof test) to 149 bar in fabrication [1]. This will have subjected the upper vessel and lower vessel, longitudinal seams, to maximum hoop stress of 273 MPa and 258 MPa respectively from equation 1.

The tensile stresses in the manway nozzle to shell weld (Joint 4, Figure 3-1) are determined by FEA are presented in Table 5-1, Section 5.1.

3.3.3 Welding Residual Stress

The welding residual stresses have a detrimental effect on fracture performance of welded joints [17]. The tensile welding residual stresses elevate the crack driving force which is used to evaluate the likelihood of fracture by comparing it with fracture toughness of the weld. Treatment of welding residual stresses in structural integrity assessment is addressed in the major standards and codes such as BS 7910 [17], API 579 / ASME FFS-1 [25] and R6 [26].

In accordance with BS 7910 [17], for welds in the as-welded condition (i.e., no post-weld heat treatment) yield magnitude residual stresses uniformly distributed across the pipe wall thickness should be assumed in the fracture assessment. However, residual stress relaxation due to proof testing is permitted in accordance with the recommendations provided in Section 7.1.10 and Annex O of BS 7910. These code recommendations were followed in the assessment of the Lower Vessel (boot).

As per the recommendation provided in BS 7910, if a structural component was subjected to the Post Weld Heat Treatment (PWHT), for a flaw in a plane parallel to the weld, the value of the residual stress can be assumed to be equal to be 20% of the lesser of the yield strengths of the weld or parent metal. The effect of the PWHT on the welding residual stress was taken into account in the fracture assessment of the Upper Vessel.

3.3.4 Cyclic Stresses

3.3.4.1 General

The scrubber is designed for natural gas (NG) operation assuming 1000 cycles at 0 to 85 barg pressure and 15000 cycles from 38 barg to 85 barg pressure [1]. The basis of this requirement is not understood and is much more onerous than expected in the vessels from previous Wood studies. Therefore, cyclic stresses predicted in the vessels over a 50-year life in hydrogen mixture service were estimated from the daily operational pressure variation actually recorded in natural gas (NG) operation.

The recorded daily operational pressure cycles for the [redacted], in NG operation, was not available at the time of writing. Therefore, pressure cycle data recorded at an adjacent NGT site was considered which was obtained from a previous Wood study for another client. The two sites are connected by a pipeline with pressure rating of 75 barg.

The method of conversion of pressure cycle data for 100% NG service to the case of 20% hydrogen or 100% hydrogen was based on that used in a previous preheating study for NGT by Wood [19] and is summarised in Section 3.3.4.2 below.

The anticipated daily pressure cycles are shown in Fig 3.2 below for 100% NG, 20% hydrogen and 100% hydrogen operation. The daily pressure variation with conversion to hydrogen is about 10.3 bar with 18250 operational cycles (1 cycle /day for 50 years) over the hydrogen mixture service.

It is expected that the scrubbers will be periodically depressurised completely (i.e. shut down) for inspection and maintenance though the frequency of such action is not clear at the time of writing. The potential effects of events on fatigue were assessed assuming annual shut down with de-pressurisation from maximum design pressure (90 bar).

The assumed pressure cycles explained above are converted to stress ranges using equation 1 for seam and girth welds with FEA being used for nozzle welds. The derived stress ranges assumed in analysis are presented in Table 5-2, Section 5.0.

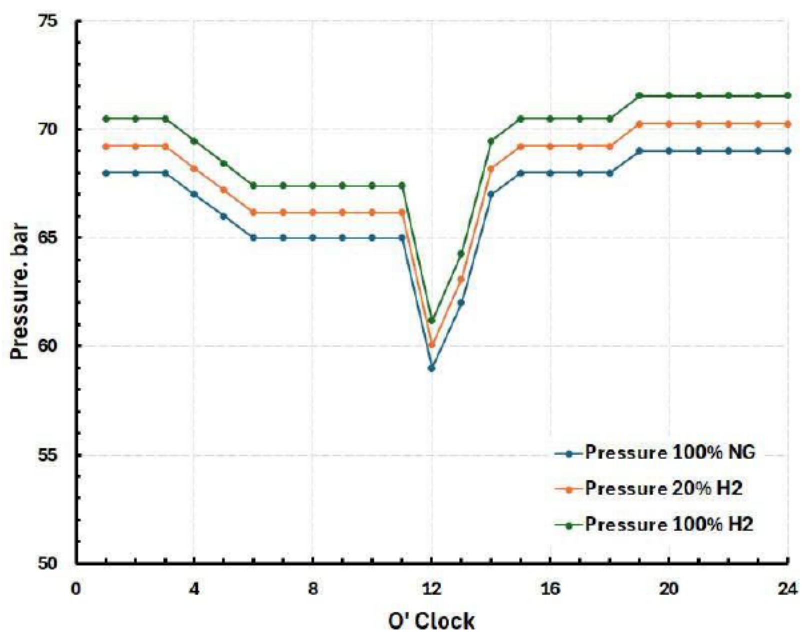

Figure 3-2 Estimated pressure cycles [redacted]

3.3.4.2 Derivation of daily pressure cycle variation for hydrogen/mixture case.

The steady-state gas network analysis was performed using Schlumberger PIPESIM 2021. The modelling approach commenced with the specified operating pressure at the delivery site for the natural gas base case and the known distance to the nearest upstream compressor station. Using these boundary conditions, the required compressor discharge pressure was back-calculated and subsequently assumed constant for all hydrogen blending scenarios. For each case, nodal flowrates were adjusted to ensure that the delivered energy demand remained equivalent to the base case of 100% natural gas operation. The flowrates for hydrogen-blended gas were determined using higher heating values (HHV), accounting for the higher mass-based heating value and lower volumetric heating value of hydrogen relative to natural gas. The resulting variations in mass and volumetric flowrates were analysed alongside network pressure behaviour. Pressure requirements at the delivery site and pressure losses across the system were evaluated as a function of blending ratio, recognising that pressure drop is governed by gas velocity and density. As hydrogen concentration increased, higher volumetric flowrates led to increased velocities, while reduced gas density influenced pressure losses, with density effects becoming increasingly significant at higher hydrogen blending levels. The main reasons for higher pressure in the case of NG operation compared to hydrogen/mixture service case are given below:

- Lower volumetric heating value of hydrogen requires higher volumetric flow rates to deliver the same energy as natural gas.
- Higher volumetric flow rates result in increased gas velocities in the pipeline.
- Increased gas velocity leads to higher frictional pressure losses along the network.
- Lower gas density of hydrogen alters hydraulic behaviour and further influences pressure loss, particularly at higher hydrogen concentrations.
- The combined effects of higher velocity and reduced density result in higher system pressure requirements compared to 100% natural gas operation.

4.0 METHODOLOGY

4.1 Stress Concentration Effect

4.1.1 Misalignment

The presence of misalignment, axial (eccentricity) or angular, or both, at a welded joint can cause an increase or decrease in stress at the joint when it is loaded, due to the introduction of local bending stresses [17]. In the current assessment, the axial and angular misalignment in the seam welds and girth welds in the vessel shell is taken into account as described below.

4.1.1.1 Seam welds – axial mislalignment

The local bending stress due to the axial misalignment (see Figure 4-1) in the seam weld is calculated as per the recommendations provided in Annex D of BS 7910 [17].

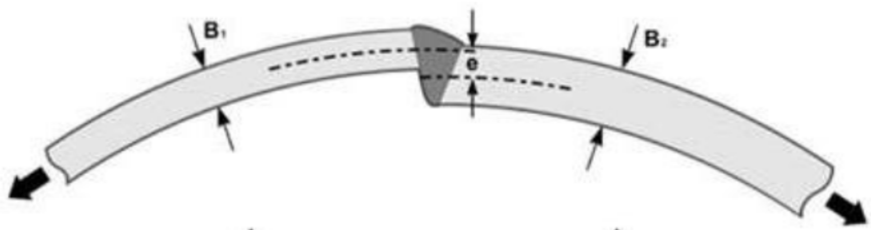

Figure 4-1 Axial misalignment of a seam weld

The bending stress component is calculated using the following equation:

$$P_b = P_m \frac{6e}{B_1(1-tJ^2)} \left[\frac{1}{1+(B_2/B_1)^{0.6}}\right] \quad (2)$$

Where:

P_m = the primary membrane stress component

P_b = the primary bending (through-thickness) stress component

e = the total centreline offset

B_1 = pipe wall thickness

B_2 = adjacent pipe wall thickness where $B_1 \geq B_2$

The assumed axial misalignment of 3 mm due to the plates offset is employed in the fatigue and fracture assessments of the seam welds in the upper vessel with the shell thicknesses of 35 mm and 40 mm (Joints 1 and 3, **Figure 3-1**). The axial misalignment of 2 mm was assumed to be present in the seam weld in the lower vessel (Joint 5, **Figure 3-1**) with the 20 mm shell thickness. The axial misalignment has resulted in the additional primary bending stress 46.74 MPa for the shell thickness 35 mm while the additional primary bending stress 35.92 MPa was estimated for the shell thickness 40 mm.

4.1.1.2 Girth welds – axial miaslignment

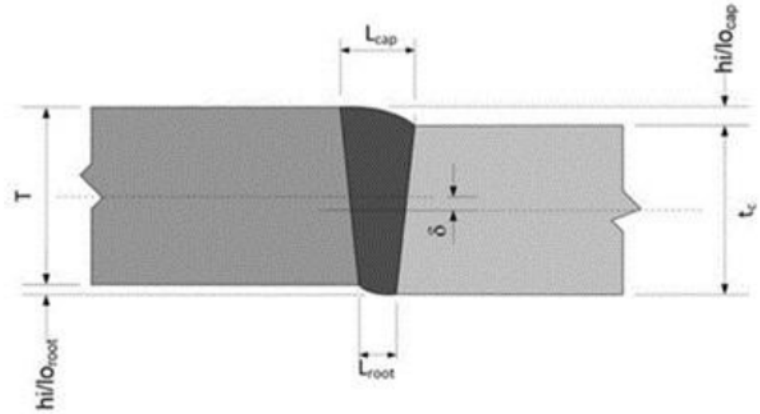

Figure 4-2 Girth weld axial misalignment – definitions

The additional through-thickness bending stress due to the axial misalignment in the girth welds was calculated as per the method recommended in DNV-RP-F108 [19]. Figure 4-3 illustrates the axial misalignment in the girth weld and provides main definition.

The stress concentration factor (SCF) at the weld cap due to axial misalignment at the girth weld is calculated using the following equation provided in DNV-RP-F108 [20]:

$$SCF = 1 + \frac{6 \cdot \delta \cdot e^{-\alpha}}{t_c \left(1 + \left(\frac{T}{t_c}\right)^{\beta}\right)} \quad (3)$$

Where

$$\alpha = \frac{1.82 \cdot L_{cap}}{\sqrt{D \cdot t_c} \cdot \left(1 + \left(\frac{T}{t_c}\right)^{\beta}\right)} \quad (4)$$

$$\beta = 1.5 - \frac{1.0}{\log\left(\frac{D}{t_c}\right)} + \frac{3.0}{\left(\log\left(\frac{D}{t_c}\right)\right)^2} \quad (5)$$

$$T = t_c + \left|hi/lo_{cap} - hi/lo_{root}\right| \quad (6)$$

$$\delta = \frac{hi/lo_{root} - hi/lo_{cap}}{2} \quad (7)$$

The SCF at the weld root is calculated as follows:

$$SCF_{root} = 1 + (SCF_{cap} - 1)\frac{L_{root}}{L_{cap}} \quad (8)$$

Where

D = outside diameter of pipe

T and t_c = wall thickness of the pipes on each side of the girth weld, $T > t_c$

δ = misalignment (wall thickness differences, out-of-roundness, centre eccentricities etc.)

L_{cap} = width of weld cap

L_{root} = width of weld root

SCF_{cap} = the SCF at the weld cap determined from Equation (2).

SCF_{root} = the SCF at the weld root determined from Equation (8).

The misalignment of 3 mm was employed in the assessment of girth welds in the upper vessel. The axial misalignment has resulted in the additional primary bending stress 18.34 MPa acting on the flaw in the girth weld.

4.1.1.3 Girth welds – angular miaslignment

Angular misalignment due to imperfect fit up in vessel seams is judged as most likely not large enough to cause a significant stress intensification but this should be confirmed by field measurement on scrubbers. However, due to the transition of the cylindrical shell to the conical shell in the upper vessel, the angular misalignment between two shell sections should be accounted in the assessment of the circumferential (girth) welds (Joint 3, Figure 3-1). The angular misalignment gives rise of the additional through-thickness bending stress component which was determined as per provisions of Annex D of BS 7910 [17].

The solution for the angular misalignment between flat plates (as illustrated in Figure 4-4) recommended in BS 7910 [17] was employed in the assessment.

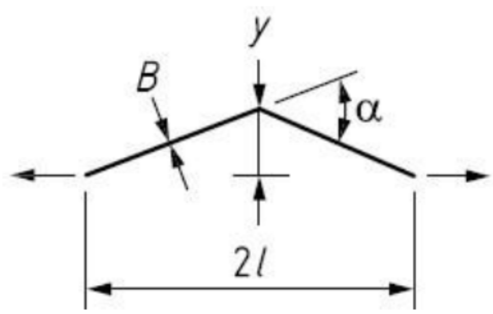

Figure 4-4 Angular misalignment between flaw plates [17]

For the fixed ends, the additional bending stress component is calculated as follows:

$$P_b = P_m \cdot \frac{3y}{B} \cdot \left[\frac{\tanh(P/2)}{P/2}\right] \quad (9)$$

Where

$$\beta = \frac{2l}{B} \cdot \Phi \frac{3\text{ఔ□a○□}}{E} \Phi^{0.S} \quad (10)$$

And

$\sigma_{max,m}$ = membrane component of the maximum applied tensile stress

E = elastic modulus

l = distance from axially misaligned joint to extremities of region of angular misalignment

B = section thickness in plane of flaw

It was found that the angular misalignment between the cylindrical and conical shells introduces the additional bending stress 43.54 MPa acting on the circumferential flaw in the girth weld.

4.1.2 Weld Toe Stress Concentration Factor

Fatigue and fracture assessment of the girth welds includes Mk factors to account for local weld toe SCF effects. Where possible the 3-D Mk solution provided in BS 7910 [17] is applied. In cases where the 3-D solution is not valid (due to crack geometry restrictions) the 2-D Mk solution provided in BS 7910 was used.

In the assessment of the internal surface breaking flaws exposed to the hydrogen environment, determination of the Mk factor is based on the in-weld cap width equal to 5 mm. The conservatism of this assumption is subject to confirmation.

4.2 Fracture Assessment

Fracture assessment of the welds in the pressure vessel is conducted using the concept of the Failure Assessment Diagram (FAD). The axes of the FAD are the plastic collapse ratio, Lr on the horizontal axis and the fracture ratio Kr on the vertical axis. The fracture ratio, Kr, is calculated by dividing the applied stress intensity factor by the material fracture toughness, while the plastic collapse ratio, Lr, is calculated by dividing the reference stress by the yield strength of the material.

BS 7910 offers several levels of treatment of flaws, depending on the application and materials data available:

- Option 1 is a conservative procedure that does not require detailed stress/strain data for the materials being analysed.
- Option 2 is based on the use of a material-specific stress-strain curve.
- Option 3 uses numerical analysis to generate FAD.

In the current assessment Option 1 procedure is utilised which uses minimum tensile properties for the material grade in question. The assessment is performed using the structural integrity assessment software Crackwise [21] which automates fracture and fatigue parts of BS 7910 [17].

An example of the FAD is shown in Figure 4-5.

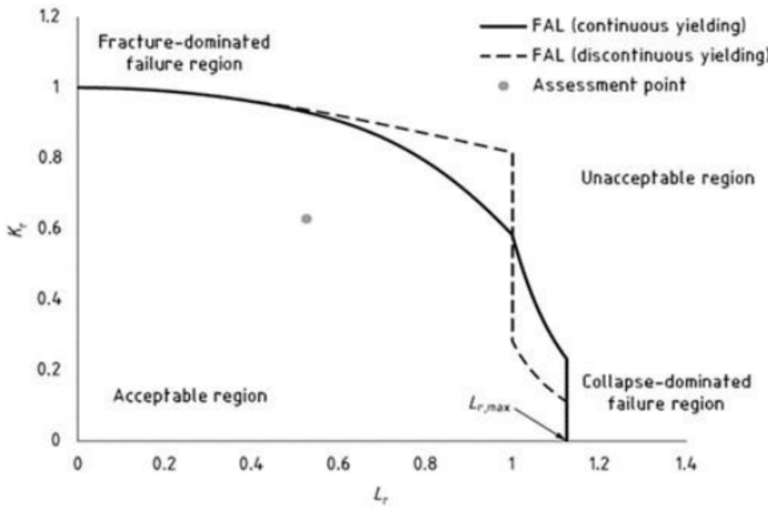

Figure 4-5 Failure Assessment Diagram

4.3 Fatigue Crack Growth Analysis

The fracture mechanics analysis accounts for fatigue loading to be imposed on the welds in operation. The fatigue assessment is performed using a fracture mechanics approach which idealises the initial flaw as a sharp tipped crack that propagates in accordance with a fatigue crack growth (FCG) law. The FCG law relates the crack growth rate (da/dN) to the range of stress intensity factor (ΔK). The stress intensity factor range, ΔK, is a function of structural geometry, stress range and instantaneous crack size. The following equation is used to predict the fatigue crack growth rate as function of the stress intensity factor range:

$$\frac{\mathrm{da}}{\mathrm{dN}} = A(\Delta K)^{\mathrm{m}} \quad (9)$$

Equation 9 which is often called as the Paris law is used in the fracture mechanics-based fatigue assessment of the pipelines.

4.3.1 Fatigue crack growth parameters – hydrogen service

It is established nowadays that the rate of fatigue crack growth in hydrogen service is significantly elevated if compared with that in air [18]. In the current study, the fatigue crack growth (FCG) law developed by Sandia National Laboratories [22] for steels in hydrogen service is used in the assessment. The two-stage Sandia fatigue crack growth law takes into account influence the stress ratio $\sigma_{\mathrm{min}}/\sigma_{\mathrm{max}}$ as well fugacity of hydrogen.

$$\text{Low } \Delta K\text{:} \frac{\mathrm{da}}{\mathrm{dN}} = 7.6x10^{-16}\left[\frac{1+0.4286\mathrm{R}}{1\text{-}\mathrm{R}}\right]\Delta K^{6.5} f^{1/2} \quad (10)$$

$$\text{Hi } \Delta K\text{:} \frac{\mathrm{da}}{\mathrm{dN}} = 1.5x10^{-11}\left[\frac{1+2\mathrm{R}}{1\text{-}\mathrm{R}}\right]\Delta K^{3.6} \quad (11)$$

Where

ΔK = the stress intensity factor range (in MPa(m)$^{0.5}$)

da/dN = the crack growth rate (in m/cycle)

f = fugacity (bar) (i.e. partial pressure of hydrogen)

R = stress ratio (minimum / maximum stress)

The lower of the two values calculated using Eq. 9 and Eq. 10 is used to construct the fatigue crack growth curve for the use in the assessment. It is demonstrated in [22, 23], Eq. 10 and Eq. 11 are intended to provide an upper bound on fatigue crack growth rates as function of both stress ratio and pressure (represented as fugacity). It is worth noting that the full-scale fatigue test data reported in [24] confirm that accelerated fatigue crack growth occurs in gaseous hydrogen. It is also stated in [24] that the magnitude of fatigue crack growth acceleration agrees well with the small-scale test data.

The hydrogen fugacity (f, partial pressure) was assumed to be 90.1 bar and 18.02 bar for 100% hydrogen and 20% hydrogen blending respectively considering operation at maximum design pressure (90 bar).

The stress ratio (R) was assumed to be 0.86 under the anticipated operating pressure cycles. This is the ratio of minimum daily operating hoop stress divided by maximum hoop stress in the pressure cycle. The predicted crack growth rate increases as the R ratio rises.

The stress ratio (R) under annual shutdowns (e.g. inspection/maintenance) is effectively zero just considering the hoop stress range with complete depressurisation to zero stress. However, higher R-ratio was assumed in assessment of shutdowns to account for the possibility that tensile weld residual stresses will effectively elevate the minimum stress in the cycles.

A stress ratio (R) of 0.2 was assumed in assessment of the upper vessel, under annual shutdowns, considering that tensile residual stresses have been reduced to 20% yield strength by PWHT (Section 3.3.3).

The stress ratio (R) of 0.86 was assumed conservatively in assessment of the lower vessel, under annual shutdowns, since it has not been subjected PWHT so will retain high residual stresses (>40% yield strength).

Constructed fatigue crack growth curves are provided in Figure 4-6. As per [22,23], if the calculated fatigue crack growth rate in hydrogen is lower than the fatigue crack growth rate in air, the fatigue crack growth rate in air shall be used. Parameters of the constructed FCG laws are summarised in Table 4-1.

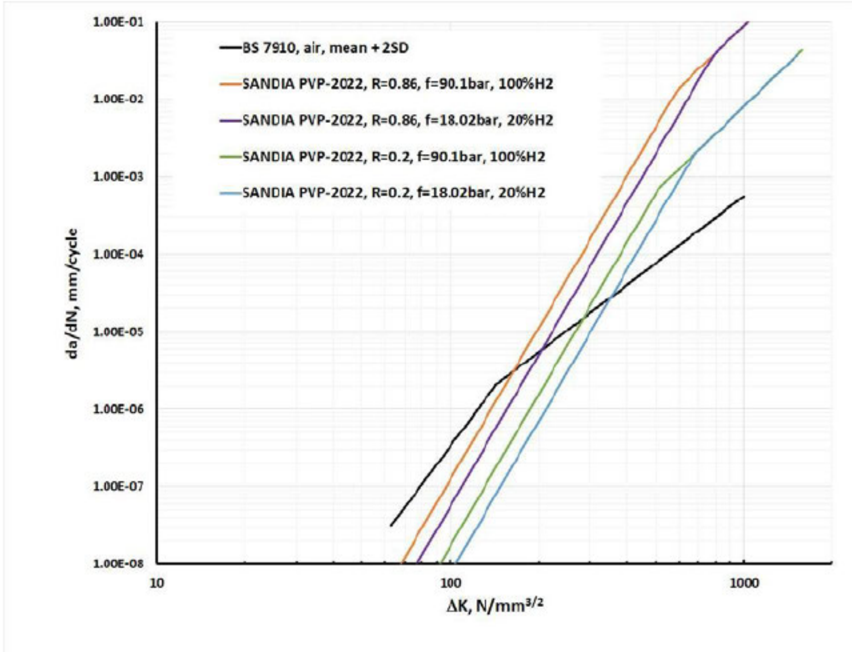

Figure 4-6 Fatigue crack growth curves constructed as per [22]

Table 4-1 Fatigue crack growth parameters – hydrogen service

H2 Pressure, bar	Stress Ratio, R	Transition Point	m	A
90.1	0.86	0	5.1	2.1E-17
		144	2.88	1.29E-12
		165	6.5	1.25407E-20
		600	3.66	9.43046E-13
90.1	0.2	0	5.1	2.1E-17
		144	2.88	1.29E-12
		285	6.5	1.74102E-21
		506	3.66	8.49433E-14
18.02	0.86	0	5.1	2.1E-14
		144	2.88	1.29E-12
		221	6.5	5.63633E-21
		791	3.66	9.43046E-13

18.02	0.2	0	5.1	2.1E-17
		144	2.88	1.29E-12
		348	6.5	7.11756E-22
		696	3.66	8.49433E-14

5.0 RESULTS AND DISCUSSION

5.1 Stress Analysis of Nozzle (Manway M1)

As explained in Section 3.2.2, the stresses for the fracture and assessment of the flaws in the longitudinal seams and circumferential (girth) welds were determined using the equation 1 (Section 3.3.2.1) above by Barlow. However, it is well known that stress fields around the nozzle to cylindrical shell connections are affected by the geometric discontinuity [27, 28]. While the analytical and semi-analytical methods for evaluating the stress concentration factors associated with the nozzle-to-shell connections are available in the literature [29, 30], they may not provide sufficient the stress field resolution to conduct fracture and fatigue assessment of the flaws which may be located in the nozzle weld. Due to this reason, a computational analysis of Manway M1 nozzle (Joint 4, **Figure 3-1**) was performed to ascertain the stresses around the largest opening in the upper vessel.

The finite element analysis of the Manway M1 was conducted using the general purpose finite element package Abaqus [31]. 3-D elastic stress analysis was performed within the finite strain (non-linear geometry) formulation. The finite element model of the nozzle on the cylindrical shell (presented in Figure 5-1) was built using 20-node brick elements to ensure sufficient stress field resolution. As shown in Figure 5-1, one end of the model was fixed while the internal pressure was applied to the inner surfaces of the shell and the nozzle. It should also be noted that the pressure thrust (end cap pressure) was applied to the nozzle and the cylinder.

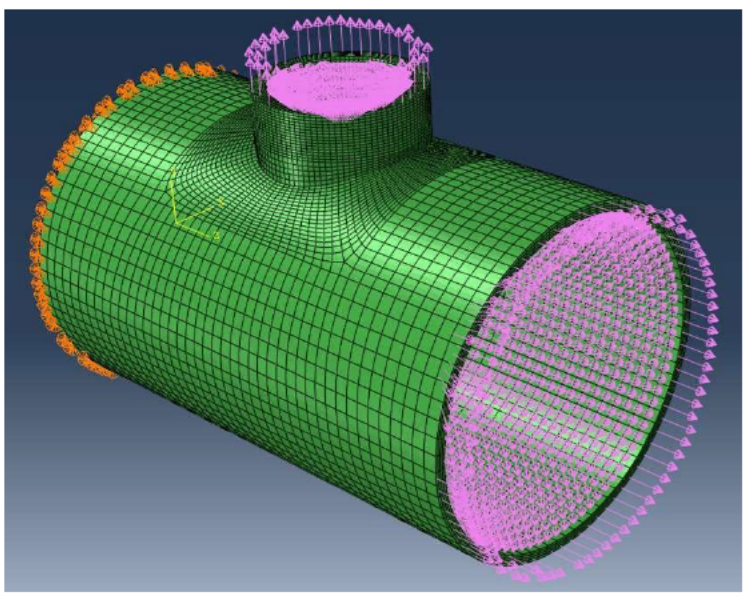

Figure 5-1 Finite element model of the nozzle-to-cylindrical shell connection

Figure 5-2 and Figure 5-3 depict distribution of the Mises and first principal stresses around the nozzle. As expected, the maximum stress level is found to be around the crotch corner. It can also be seen in Figure 5-4 where the distribution of the first principal stress around the crotch corner is presented.

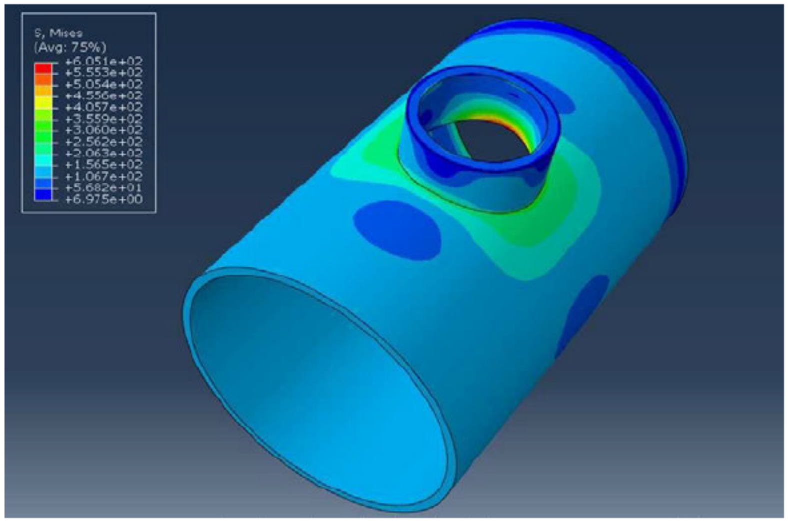

Figure 5-2 Mises stress distribution around the nozzle-to-shell connection

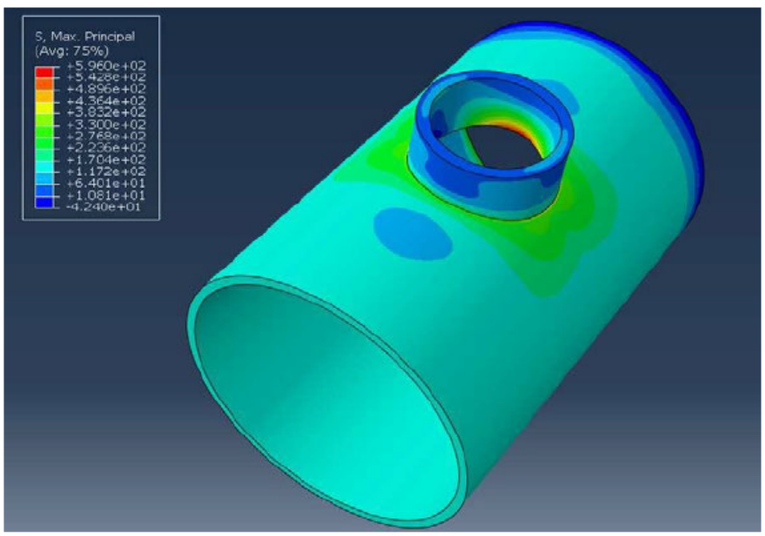

Figure 5-3 First principal stress distribution around the nozzle-to-shell connection

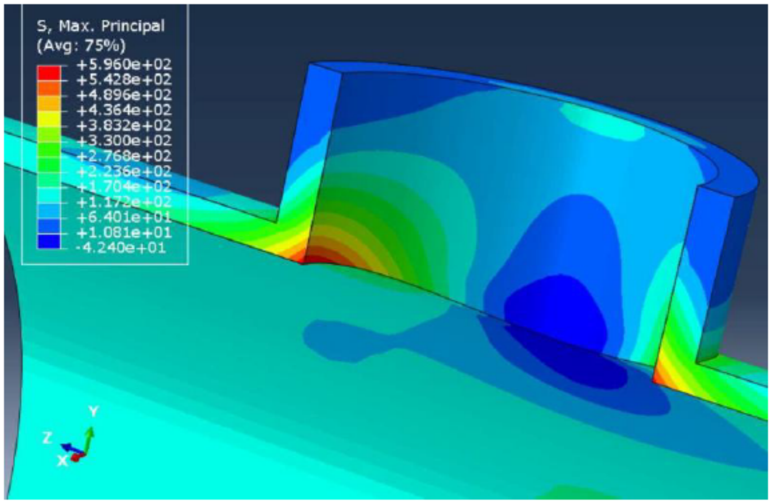

Figure 5-4 First principal stress distribution at the crotch corners

Together with the magnitude of the first principal stress, it is also important to ascertain the first principal stress orientation with respect to the plane of potential crack-like flaw. Figure 5-5 shows vectors of the first principal stress as well as planes of the potential lack-of-fusion (LoF) flaws in the nozzle weld. It can be seen that the first principal stress does not act as the opening mode stress for the LoF flaws. Therefore, the longitudinal stress (i.e. (stress component parallel to vessel axis) was obtained in the post-processing of the FEA results to facilitate the assessment of the potential LoF flaws in the nozzle weld.

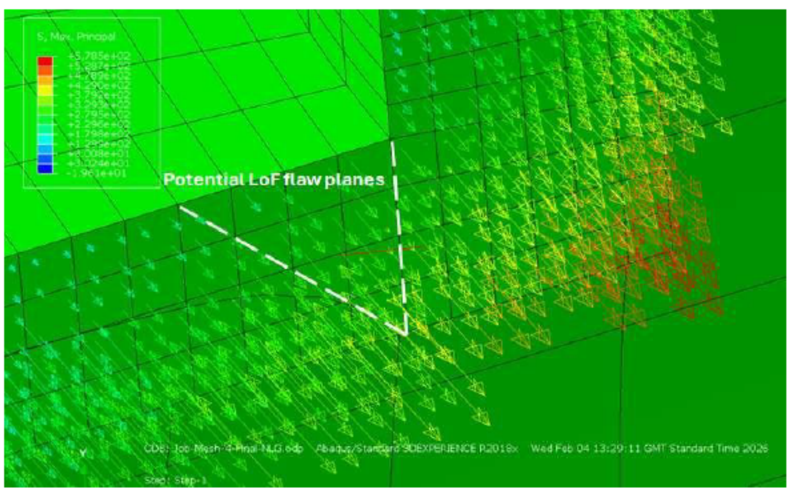

Figure 5-5 Vectors of the first principal stress in the crotch corner

Figure 5-6 and Figure 5-7 provide contour plots of the longitudinal stress (S33 component) and the first principal stress together with the stress categorisation lines for the LoF flaws as well as the crotch corner flaw. It can be seen that, the stress categorisation lines follow the planes of the flaws to be considered in the assessment. The stress linearisation to obtain the membrane and bending stresses for the assessment was performed as per the recommendation provided in ASME Section VIII Division 2 [33] using the tool implemented in the general purpose finite element package Abaqus.

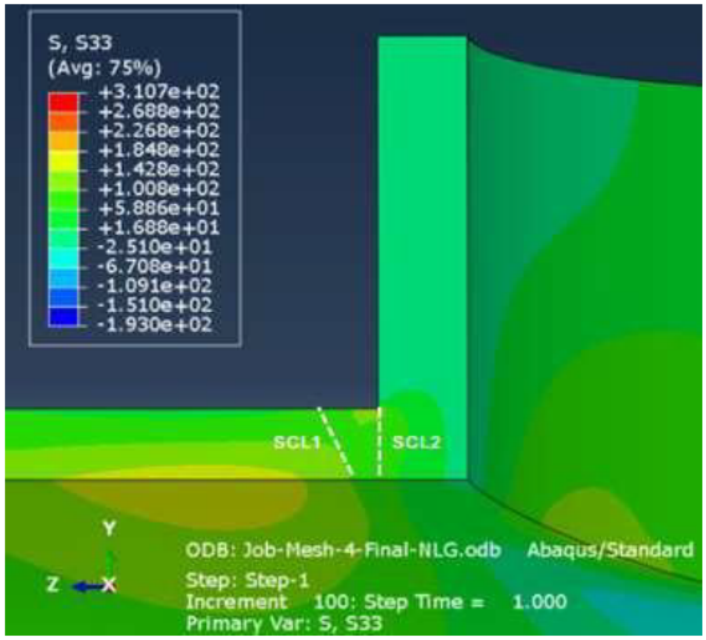

Figure 5-6 Distribution of the longitudinal stress (S33) and the stress categorisation lines for the assessment of the LoF flaws in the nozzle-to-shell weld

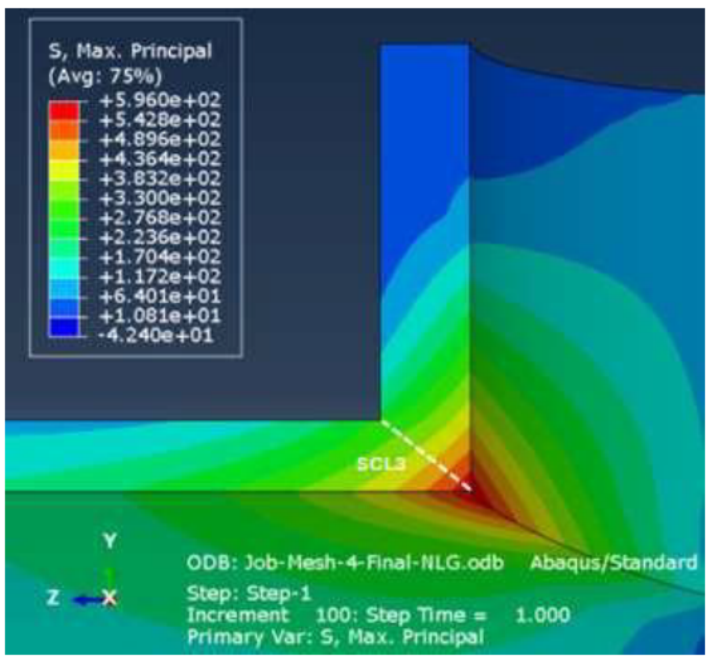

Figure 5-7 Distribution of the first principal stress and the stress categorisation line for the assessment of the crotch corner flaw

Table 5-1 provides results of the stress linearisation along the selected stress categorisation lines. It can be seen that a potential flaw at the crotch corner would be subject to the highest stresses due to the stress concentration at the geometrical discontinuity. The membrane and bending stress components were used in the structural integrity assessment software package Crackwise.

Table 5-1 Linearised stresses for the fracture assessment of many way nozzle weld. Joint 4, Figure 3-1 .Figure 3-2

Stress Categorisation Line	Membrane Stress, MPa	Bending Stress, MPa
SCL-1 (LoF Flaw)	103.17	33.88
SCL-2 (LoF Flaw)	106.56	33.94
SCL-3 (Crotch Corner Flaw)	450.46	141.92

5.2 Fracture Assessment

Fracture assessment of the seam and girth welds as well as the nozzle-to-shell weld in the manway M1 in the upper vessel and the seam weld in the lower vessel was carried out as per the methodology outlined in Section 4.

5.2.1 Upper Vessel

5.2.1.1 Seam welds

The fracture assessment of the seam welds in the vessel was performed considering two wall thicknesses: 40 mm in the cylindrical section (Joints 1, Figure 3-1) of the shell and 35 mm in the conical section (Joint 2, Figure 3-1) of the shell. As the upper vessel was subjected to the PWHT, the welding residual stress in the vessel can be taken as equal to 20% of the parent material yield strength as per the provision of BS 7910 [17].

As per Table **3-4**, the internal surface flaw 3 mm x 20 mm was considered in the assessment of the seam weld in the cylindrical section of the shell with the thickness of 40 mm while the internal flaw 3 mm x 17.5 mm was considered in the assessment of the conical section of the vessel shell with the thickness of 35 mm.

The assessment results presented in Figure 5-8 within the framework of the Failure Assessment Diagram (FAD) indicate that integrity of the seam weld exposed to hydrogen environment will not be compromised even if the fracture toughness of the weld is as low as 40 $MPa\sqrt{m}$.

Figure 5-9 presents integrity envelopes (the maximum allowable flaw heights vs. flaw length) constructed for the fracture toughness values of 40 $MPa\sqrt{m}$ and 55 $MPa\sqrt{m}$. The allowable flaw size (Figure 5-9) far exceeds the UT acceptance criteria in scrubber fabrication (Section 3.2.3). It can be seen that increase in the fracture toughness significantly expands the safety margin for the flaws considered in the assessment.

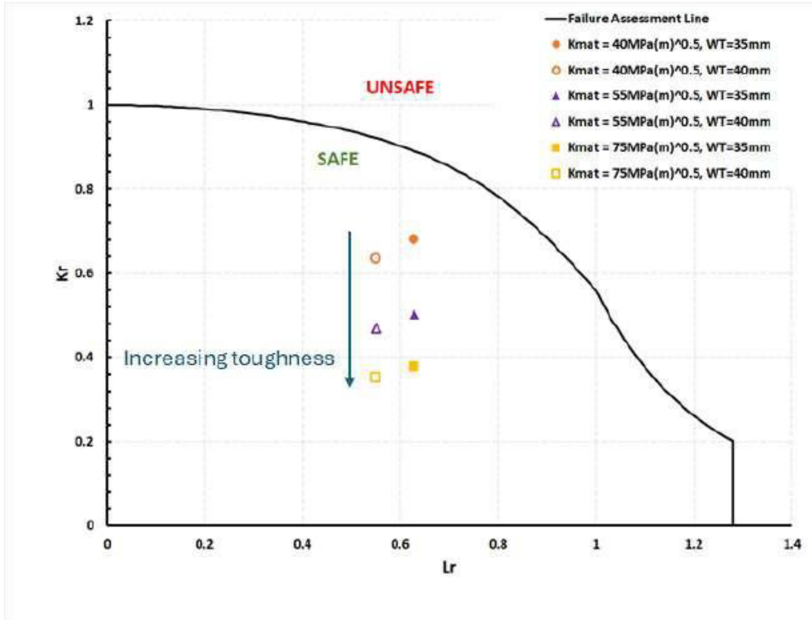

Figure 5-8 Fracture assessment of the seam weld in the upper vessel within the FAD framework.

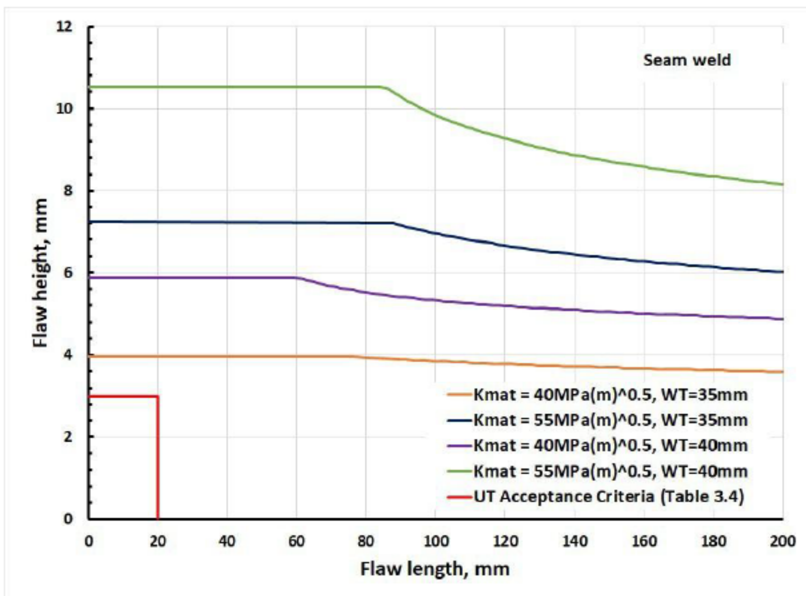

Figure 5-9 Integrity envelopes for the seam weld in the upper vessel

5.2.1.2 Girth Weld

The fracture assessment of the circumferential (girth) weld in the upper vessel (Joint 3, Figure 3-1) was performed considering the weld thicknesses of 35 mm which represents the wall thickness in the conical section of the shell. It should also be noted that in the addition to the axial alignment, the angular misalignment at the transition between the cylindrical and conical section of the shell was considered in the assessment.

As per Table **3-4**, the internal surface flaw 3 mm x 17.5 mm was considered in the assessment of the girth weld. The assessment results presented in **Figure** 5-10 within the framework of the Failure Assessment Diagram (FAD) indicate that integrity of the girth weld in hydrogen environment will not be compromised even if the fracture toughness of the weld is found to be as low as 40 MPa√m.

Figure 5-11 presents integrity envelopes (the maximum allowable flaw heights vs. flaw length) constructed for the fracture toughness values of 40 MPa√m and 55 MPa√m. The allowable flaw size (

Figure 5-11) far exceeds the UT acceptance criteria in scrubber fabrication (Section 3.2.3). It can be seen that a significant safety margin exits for the flaw 3 mm x 17.5 mm assumed to be present in the girth weld.

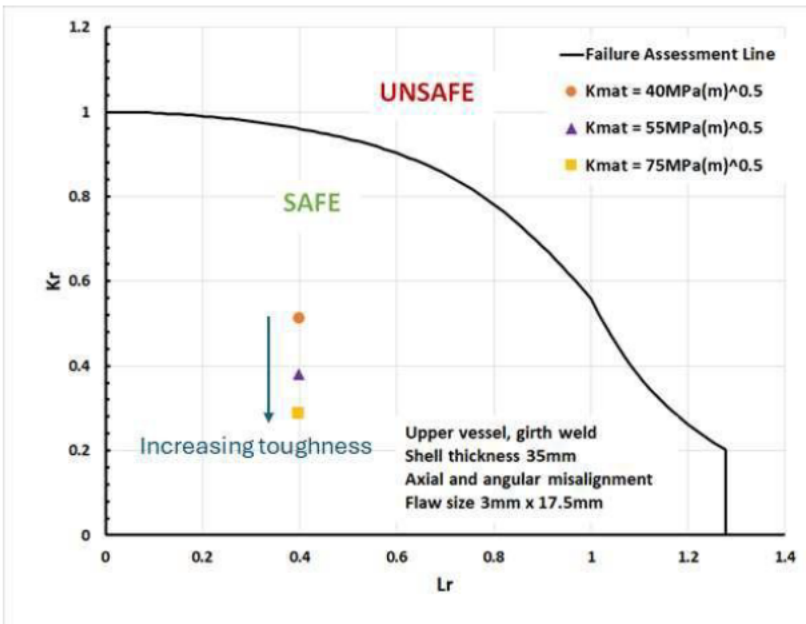

Figure 5-10 Fracture assessment of the girth weld in the upper vessel within the FAD framework.

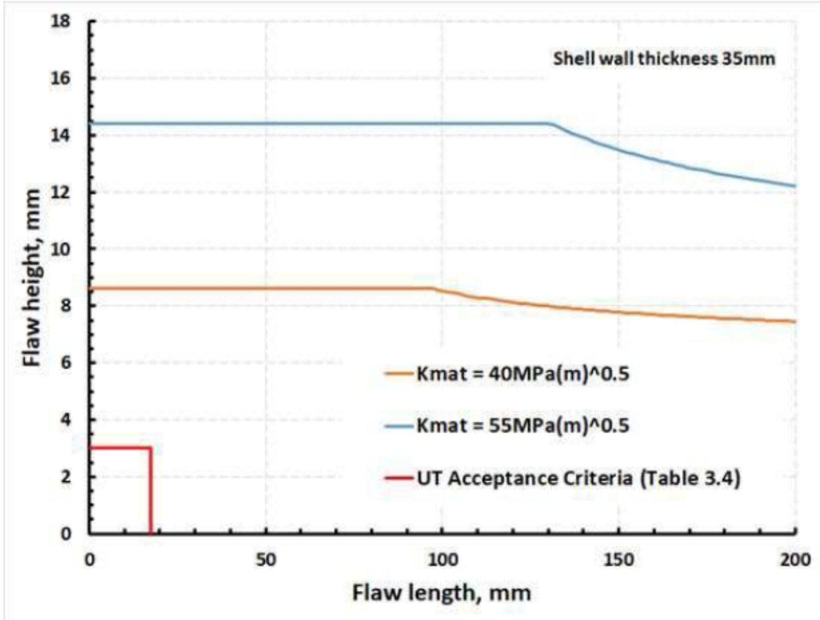

Figure 5-11 Integrity envelopes for the girth weld in the upper vessel

5.2.1.3 Nozzle Weld (Manway M1)

The fracture assessment of the nozzle weld (Joint 4, Figure 3-1, Manway M1) in the upper vessel was conducted considering two locations of potential lack-of-fusion defects as illustrated in Figure 5-6. The assessment was performed using the membrane and through-thickness bending stress components obtained from the finite element stress analysis (FEA) as outlined in Section 5.1.

Figure 5-12 depicts results of the assessment of the flaw of the size 3 mm x 20 mm (Table 3.4) in the nozzle weld at the fusion line between the shell and the weld metal (the stress categorisation line SCL-1 as per Figure 5-6). It can be seen that that integrity of the nozzle weld in hydrogen environment will not be compromised even if the fracture toughness of the weld is as low as 40 MPa√m.

Figure 5-13 presents integrity envelopes (the maximum allowable flaw heights vs. flaw length) constructed for the fracture toughness values of 40 MPa√m, 55 MPa√m and 75 MPa√m. It can be seen that a significant safety margin exits for the flaw 3 mm x 20 mm assumed to be present in the nozzle weld at the fusion line between the shell and the weld metal. The allowable flaw size (

Figure 5-13, Figure 5-8) far exceeds the UT acceptance criteria in scrubber fabrication (Section 3.2.3).

Figure 5-14 provides results of the assessment of the flaw of size 3 mm x 25 mm in the nozzle weld at the fusion line between the nozzle pipe and the weld metal (the stress categorisation line SCL-2 as per Figure 5-6). It can be seen that that integrity of the nozzle weld in hydrogen environment will not be compromised even if the fracture toughness of the weld is as low as 40 MPa√m.

Figure 5-15 presents integrity envelopes (the maximum allowable flaw heights vs. flaw length) constructed for the fracture toughness values of 40 MPa√m, 55 MPa√m and 75 MPa√m. It can be seen that a significant safety margin exits for the flaw 3 mm x 20 mm assumed to be present at the fusion line in the weld between the nozzle pipe and the weld metal. The allowable flaw size (Figure 5-15) far exceeds the UT acceptance criteria in scrubber fabrication (Section 3.2.3).

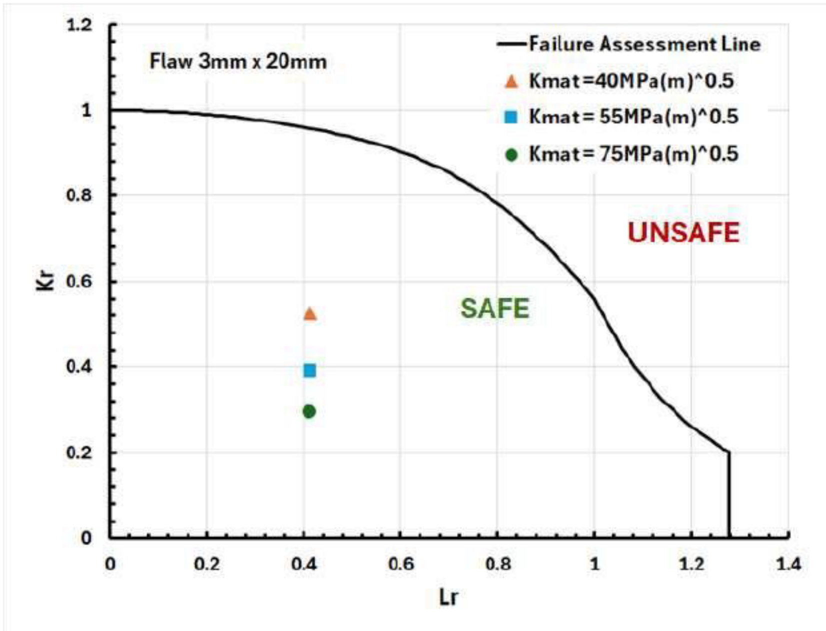

Figure 5-12 Fracture assessment of the LoF Flaw, SCL-1. The chart shows FAD points for 3mm x 20mm size flaw assuming different toughness levels ($K_{mat,H}$).

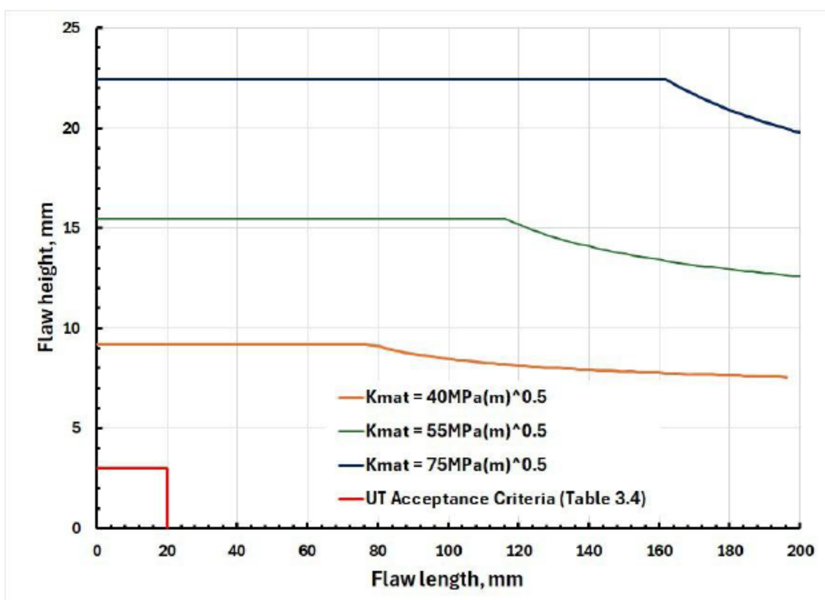

Figure 5-13 Integrity envelopes for the LoF flaw, SCL-1

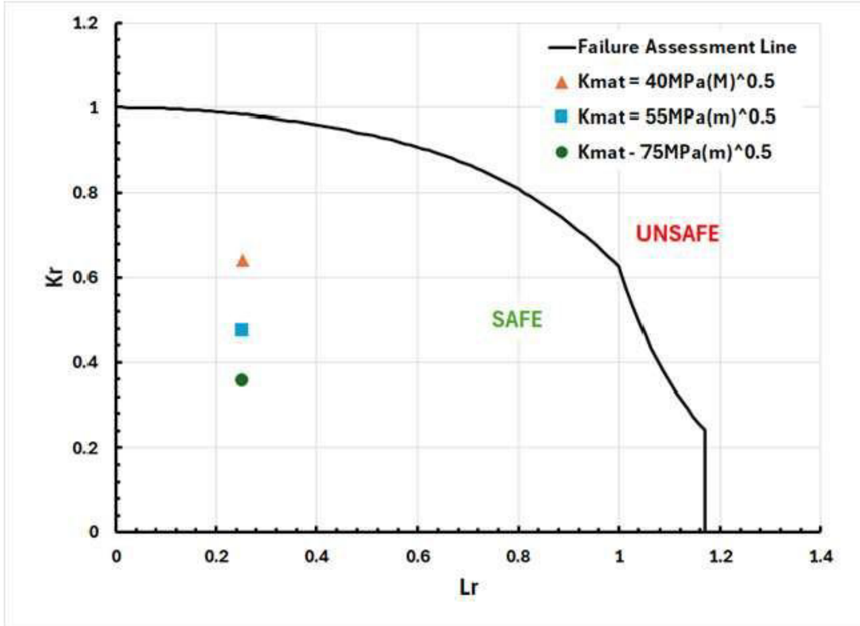

Figure 5-14 Fracture assessment of the LoF Flaw, SCL-2. The chart shows FAD points for 3mm x 25mm size flaw assuming different toughness levels ($K_{mat,H}$).

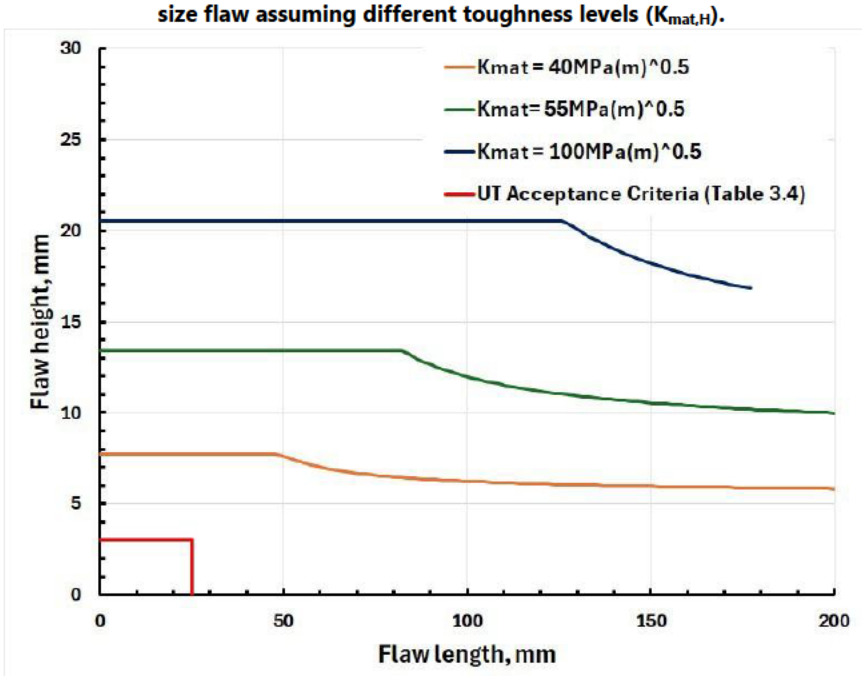

Figure 5-15 Integrity envelopes for the LoF flaw, SCL-2

An additional assessment was performed assuming presence of a flaw at the crotch corner of the nozzle. As confirmed in the stress analysis described in Section 5.2, there is a significant stress elevation around the crotch corner due to the geometrical discontinuity. The corner flaw 3 mm x 10 mm was considered in the assessment. However, it should be noted that this area is parent plate, rather than weld, so it is expected to be free from crack-like flaws formed in manufacture or fabrication.

The assessment results presented in Figure 5-16 within the framework of the Failure Assessment Diagram indicate that the fracture toughness of 110 $MPa\sqrt{m}$ is required to ensure integrity of the nozzle in the hydrogen environment. This toughness requirement far exceeds the level which can be demonstrated by FM test in hydrogen pressure environments (Section 3.2.2.2). The prediction highlights the need for the inspection of the nozzle using the reliable methods of NDT to demonstrate absence of the crack-like flaws in the highly stressed area of the nozzle.

It should be noted that areas subjected to high strain at stress concentrations in hydrogen gas environments have an increased susceptibility to crack initiation due to the effect of the environment in reducing ductility. However, the fact the crotch corner material has been pre-strained in the hydrotest is expected to diminish this threat.

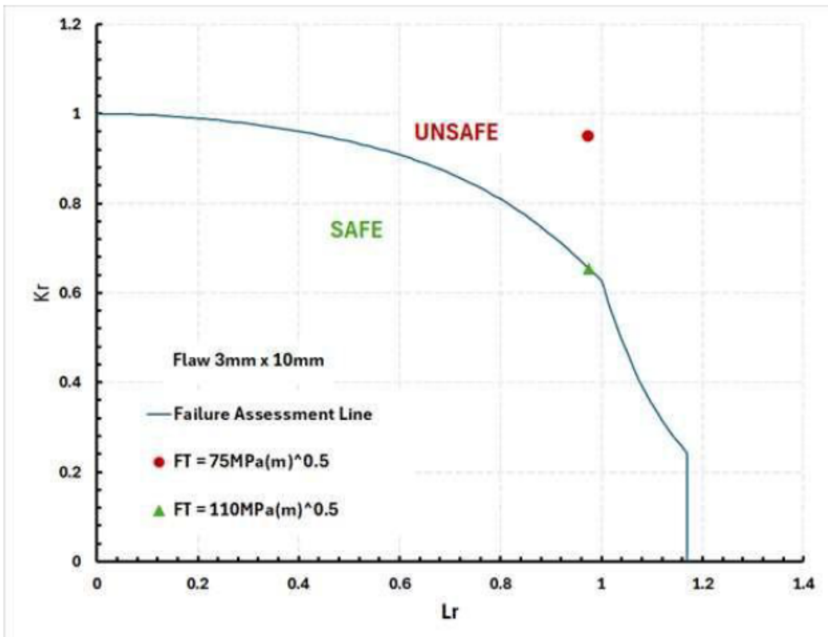

Figure 5-16 Fracture assessment of the crotch corner flaw, SCL-3. The chart shows FAD points for 3mm x 10mm size flaw assuming different toughness levels ($K_{mat,H}$).

5.2.2 Lower Vessel

Fracture assessment of the seam weld in the lower vessel was performed using the methodology outlined in Section 4. The assessment of the seam weld was conducted assuming presence of an internal surface breaking flaw of the size 3 mm x 10 mm (Table 3.4). It should be noted that the main differentiator between the conditions of the upper vessel and the lower vessel is the fact that post weld heat treatment (PWHT) was not applied in the latter case.

As the lower vessel was not subjected to the PWHT, the presence of the welding residual stress of the magnitude equal to the yield strength of the shell material was taken into account in the assessment. Following the recommendations provided in Annex O of BS 7910 [17], relaxation of the welding residual stress due to the applied stress due to hydrotest was taken into the consideration.

Figure 5-17 illustrates the assessment of the seam weld in the lower vessel containing the internal axial flaw 3 mm x 10 mm within the framework of the Failure Assessment Diagram. As expected, the welding residual stress significantly elevates the crack driving force resulting in the more onerous requirements to the fracture toughness of the weld in hydrogen environment. It can be seen from Figure 5-17, that integrity of the seam weld containing the internal axial flaw 3 mm x 10 mm will be compromised if the fracture toughness of the weld in hydrogen environment is found to be equal to 40 $MPa\sqrt{m}$.

Figure 5-18 provides integrity envelopes for the seam weld in the lower vessel constructed for three fracture toughness values: 40 $MPa\sqrt{m}$, 55 $MPa\sqrt{m}$ and 75 $MPa\sqrt{m}$. It can be seen that there is a small safety margin if the axial flaw 3 mm x 10 mm is present in the seam weld with the fracture toughness 55 $MPa\sqrt{m}$ which is typically achievable in testing carbon steel linepipe and welds.

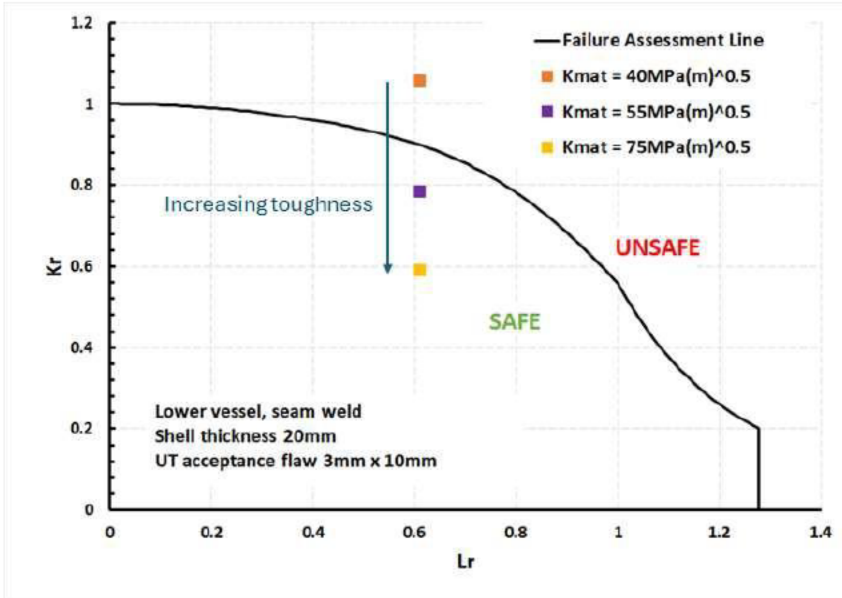

Figure 5-17 Fracture assessment of the seam weld in the lower vessel within the FAD framework.

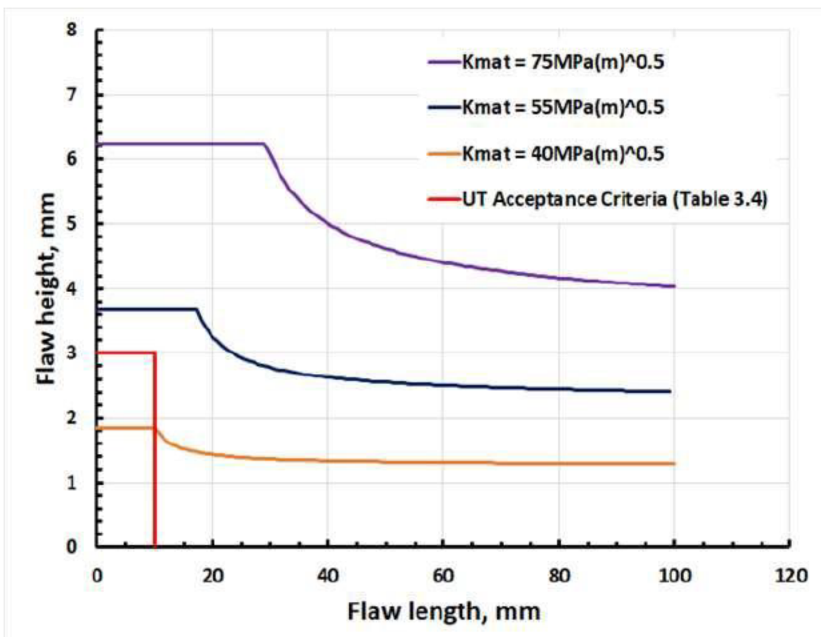

Figure 5-18 Integrity envelopes for the seam weld in the lower vessel

5.3 Fatigue Crack Growth Assessment

Fracture mechanics based fatigue assessment of the welds in the upper and lower vessels was performed considering operational pressure fluctuations (Fig 3.2) and associated stress ranges (Section 3.3.4). Further analysis assessed 50 annual shutdowns with complete de-pressurisation from the maximum design pressure 90.1 bar

(Section 3.3.4). The assessment was performed using the fatigue crack growth laws presented in Section 4.3.1 for 20% hydrogen and 100% hydrogen.

5.3.1 Assessment Results – Operational Pressure Cycles

In operating case assessment, it was considered that the upper and lower vessels will be subjected to 18250 operational cycles in the intended life of 50 years (1 cycle/day). The fatigue crack growth assessment was performed for the seam welds in the upper and lower vessels as well as considering the lack-of-fusion flaws in the nozzle M1 (manway) in the upper vessel. The stress ranges employed in the base case fatigue crack growth assessment are summarised in Table 5-2.

[redacted]

Results of the assessment of operational pressure cycles are summarised in Table 5-3. It can be seen that the cyclic stresses associated with the daily pressure fluctuations do not induce any growth of the considered flaws due to fatigue. Therefore, it can be concluded that integrity of the vessels will be controlled by resistance to fracture under static stress.

Table 5-3 Summary of the fatigue crack growth assessment – Operational pressure cycles

Weld Location	Initial Flaw size, mm x mm	End-Of-Life Flaw Size, 20% H_2, mm x mm	End-Of-Life Flaw Size, 100% H_2, mm x mm
Upper Vessel, Seam Weld, WT=40 mm	3.0 x 20.0	3.0 x 20.0	3.001 x 20.001
Upper Vessel, Seam Weld, WT=35 mm	3.0 x 17.5	3.0 x 17.5	3.001 x 17.503
Upper Vessel, Nozzle, LoF, SCL-1	3.0 x 20.0	3.0 x 20.0	3.0 x 20.0
Upper Vessel, Nozzle, LoF, SCL-2	3.0 x 25.0	3.0 x 25.0	3.0 x 25.0
Lower Vessel Seam Weld, WT=20 mm	3.0 x 10.0	3.0 x 10.0	3.0 x 10.005

5.3.2 Assessment Results – Annual Shutdown

An additional assessment was performed based on the hypothesis that the scrubber could be subjected to full depressurisation cycles associated with annual shutdowns for maintenance and repair over the 50 years hydrogen mixture service (Section 3.3.4.1). The fatigue crack growth (FCG) assessment was performed for both 20% hydrogen and 100% hydrogen. As indicated in Section 4.3.1, the stress ratio R of 0.2 was considered in the assessment of the upper vessel subjected to the PWHT while the stress ratio R of 0.86 was considered for the lower vessel since it was as welded (no PWHT).

The results are presented in Table 5-4 below. It can be seen that 50 shutdowns are not predicted to induce additional fatigue crack growth in the welds of the upper vessel. Therefore, integrity of the upper vessel is governed by fracture resistance of the welds subjected to static pressure loads.

Table 5-4 Summary of the fatigue crack growth assessment – Annual shutdown over 50 years.

Weld Location	Initial Flaw size, mm x mm	End-Of-Life Flaw Size, 20% H_2, mm x mm	End-Of-Life Flaw Size, 100% H_2, mm x mm
Upper Vessel, Seam Weld, WT=40 mm	3.0 x 20.0	3.07 x 20.14	3.09 x 20.17
Upper Vessel, Seam Weld, WT=35 mm	3.0 x 17.5	3.06 x 17.68	3.08 x 17.7
Upper Vessel, Nozzle, LoF, SCL-1	3.0 x 20.0	3.005 x 20.01	3.01 x 20.02
Upper Vessel, Nozzle, LoF, SCL-2	3.0 x 25.0	3.005 x 25.01	3.01 x 25.01
Lower Vessel Seam Weld, WT=20 mm	3.0 x 10.0	3.16 x 12.27	3.4 x 13.01

However, a limited fatigue crack growth is predicted for the seam weld in the lower vessel if subjected to 50 shutdowns. Much more fatigue crack growth is predicted in the lower vessel, compared to the upper one, since it has not been subjected to relief of residual stresses by PWHT resulting in higher R ratio and more onerous FCG law (Section 4.3.1). However, the predicted fatigue crack growth is insignificant for practical purposes (≤0.4 mm).

Figure 5-19 shows integrity envelopes constructed for different fracture toughness values together with the initial and the end-of-life flaw sizes. It can be seen that the fracture toughness of 55 $MPa\sqrt{m}$ is sufficient to ensure integrity of the seam weld in the lower vessel throughout the intended hydrogen service.

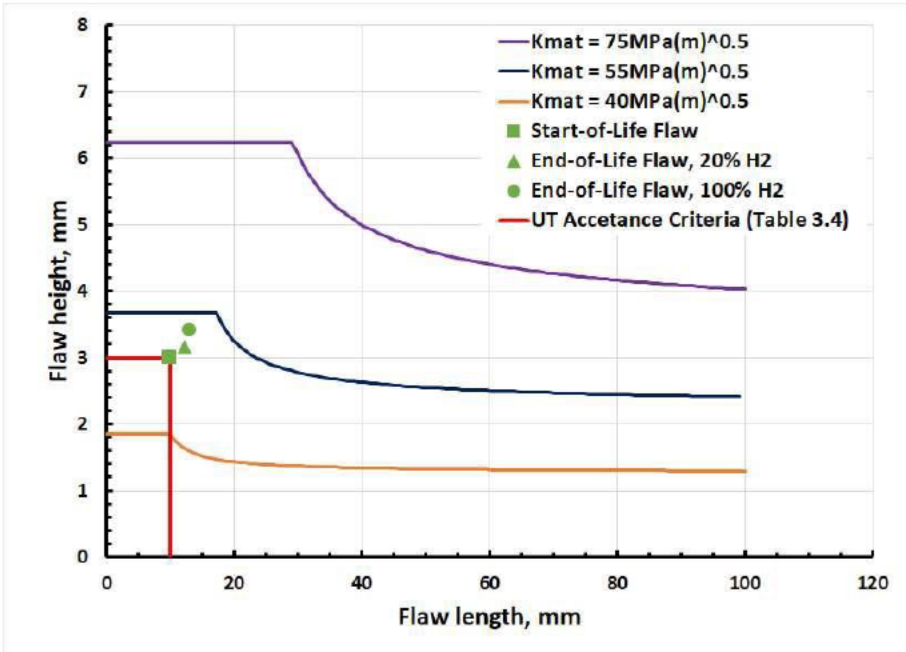

Figure 5-19 Integrity envelopes for the seam weld in the lower vessel and the predicted end-of-life flaws

6.0 CONCLUSIONS AND RECOMMENDATIONS

6.1 Conclusions

The below conclusions are made regarding the acceptability of the joints assessed in [redacted] scrubber (Figure 3-1), under anticipated cyclic and static tensile stresses, in terms of cracking resistance in future hydrogen/mixture service.

The conclusions are based on comparison of the allowable (critical) crack sizes predicted by the FM approach with largest sizes expected in the welds considering the acceptance criteria for ultrasonic testing (UT) in the scrubber fabrication.

1. The allowable flaw size is governed by resistance to crack propagation under static stress (toughness) in the hydrogen environment rather than fatigue crack growth due to cyclic stress which is insignificant.
2. Longitudinal seam welds and circumferential (girth) welds in the main (upper vessel) (Joints 1,2 and 3, Figure 3-1) are acceptable even with flaws exceeding the UT acceptance criteria limits and with a lower bound assumption regarding toughness in hydrogen ($40\ \mathrm{MPa}\sqrt{\mathrm{m}}$) (Figure 5-9 and 5-11).
3. Welds connecting the manway nozzle to main shell (Joint 4, Figure 3-1) are acceptable even with flaws far in excess of the UT acceptance criteria limits and a pessimistic assumption regarding toughness in hydrogen ($40\ \mathrm{MPa}\sqrt{\mathrm{m}}$) (Figure 5-13 and 5-15). .
4. The manway nozzle (Joint 4, Figure 3-1) crotch corner is predicted to be subjected to high stress concentration (Figure 5-4) rendering it crack sensitive with allowable flaw size well below NDT criteria. However, this area is parent material so would not be expected to contain pre-existing crack-like flaws from manufacturing to propagate.
5. Seam welds in the lower vessel (Joint 5, Figure 3-1) are acceptable though the margins of acceptability against UT acceptance criteria are more restricted (Figure 5-18). This is subject to meeting a minimum toughness $55\ \mathrm{MPa}\sqrt{\mathrm{m}}$ in testing in hydrogen which is normally achievable in testing carbon steel linepipe.
6. Based on the above (1 to 5), it is concluded that the FM analysis indicates that the scrubbers can be proven to be crack resistant in future hydrogen/mixture service by the FM approach. This is subject to confirmation that the assumptions are conservative by further NDT, stress analysis and also material testing in hydrogen of redundant scrubbers if necessary as explained below (Section 6.2). It is expected that this further work will confirm cracking resistance for the upper vessel and probably also for the lower vessel though the outcome is less certain.
7. The conclusion and recommendations of this report are largely applicable to other scrubbers for which detailed information has been obtained (**Table 3-1** above) with similar design, steel grades and stress levels. An exception is [redacted] scrubber, in the conical head area (See Section 6.2, Item 6), since it is subjected to much higher stress compared to the other scrubbers.

6.2 Recommendations

The below further work is recommended in order to confirm vessel acceptability for hydrogen/mixture service.:

1. The scrubber should be subjected to inspection using advanced NDT methods with proven reliability to detect and size crack-like (planar) flaws in vessel seams and nozzle welds. Some phased array ultrasonic methods are understood to have this capability but may need to be supplemented by additional surface inspection methods such as eddy current or fluorescent MPI. The advanced NDT may be conducted

opportunistically together with the routine shut down for maintenance and inspection. The FM analysis indicates that the most crack sensitive areas requiring focus for inspection and manway nozzle crotch corner (Figure 5-5, Figure 3-1 Joint 4) and lower vessel (Figure 3-1).

2. The fatigue assessment is based on daily operating pressure cycles recorded in another adjacent asset and assuming that depressurisation for inspection/maintenance only occurs once a year. The conservatisms of this assumption should be confirmed.

3. The welds assessed in this study (Figure 3-1, Joints 1 to 5) were selected based on judgement that they are subjected to the most onerous stresses. This should be confirmed in further work to determine the stress concentrating effect at the small diameter (2 inch OD) set on nozzles (e.g. Joint 6, Figure 3-1) and nozzle connecting the upper vessel to lower vessel (Joint 7, Figure 3-1).

4. There is reasonable confidence that a minimum toughness level exceeding 55 MPa√m would be demonstrated in testing the steel and welds of the scrubbers (Section 3.2.2.2) in hydrogen. However, this should be confirmed by tests on representative pressure vessel steel and welds perhaps obtainable from redundant NGT scrubbers. The degree of necessity for this testing depends on the results of the NDT (Item 1) and the size of any flaws detected which need to be justified. For example, if the reliable advanced NDT detects no flaws or only minor discontinuities then in some cases it may be justifiable not to conduct toughness testing in hydrogen.

5. As explained in the previous study [9] complete manufacturing records and as built information were not received for the scrubbers identified except for the one [redacted] Therefore, field investigation should be conducted to confirm steel composition, hardness and microstructure using non-destructive methods.

6. Further stress and FM analysis is required to determine suitability of [redacted] scrubber for hydrogen/mixture service since it is characterised by much higher hoop stresses compared to [redacted] scrubber assessed. The elevated stresses are in the conical head (44 mm thickness) and butt weld connecting it to the main can (76 mm thickness) which will be subjected to a high stress concentration due to the thickness change.

8. This study only covered the scrubber at [redacted] for which sufficient information has been obtained (**Table 3-1**) for FM analysis. Further survey of the scrubbers at other NGT sites should be made to clarify their key characteristics (design, dimensions, stress levels, steel grades, PWHT extent) and compare to the **Table 3-1** above. In this way the transferability of the results of this study to all the other scrubbers of the network can be clarified and the need for further stress and FM analysis of additional example scrubbers determined.

9. Based on the above (Item 7), a scope of work to cover all the scrubbers in the network should be developed defining the required stress analysis, FM analysis and NDT.

10. The cost of FM analysis, associated stress analysis and NDT should be estimated and compared with the alternative option of replacement with new scrubbers. The latter may be justified as hydrogen ready by conformance with ASME VIII, Division 3, Article KD-10 [32]. This is subject to confirmation of reliability in hydrogen/mixture service by vendor product operating experience and the FM approach may still be required even if not mandatory according to ASME code [32]. All new scrubbers should be subjected to PWHT since this increases resistance to cracking in hydrogen environments.

7.0 References

1. Glapwell, General Arrangement of 2 Phase Gas Scrubbers, 3 off as drawn, Equipment Tag numbers: [redacted] Pipeline Ltd, Drawing number : 4221/1
2. Peerless Europe limited, 2.75M ID Peerless Horizontal, SWRL Tube Separator, , Drawing: 21/2078/0008 SHT 1, Rev 1 . Peerless Ref No: 02/2078/26, 06 Feb 2003
3. Wefco (Gainsborough) Limited, 2 Off scrubber vessels, equipment numbers -Vessels 1,2 Fabrication Detail, Drawing: 26892/01, 25 April, 2018
4. PD 5500 2024 +A1 2024 Specification for unfired pressure vessels, BSI Standards Publication
5. BSI BS 1501-1 - Steels for Pressure Purposes - Part 1: Specification for Carbon and Carbon Manganese Steels: Plates
6. ASTM A333/A333M-24. Standard Specification for Seamless and Welded Steel Pipe for Low-Temperature Service and Other Applications with Required Notch Toughness
7. Characteristics of Hydrogen and Natural Gas Blends in the NTS: Phase 1, Wood, Prepared for National Gas Transmission, Document:809337-00-PR-REP-0001, 26/09/2023
8. Characteristics of Hydrogen and Natural Gas Blends in the NTS, Wood, Prepared for National Gas Transmission, Document: 809337-00-PR-REP-003, 27/05/2024
9. Impact of Hydrogen on Gas cleaning Assets-WP1: Evaluation of current gas cleaning asset capability with hydrogen and blends, Prepared for National Gas Transmission, Rev 02, 810389-00-PR-REP-0001, December 2024
10. NTS Materials Pipeline Assessment, Project NIA_NGT0244, https://smarter.energynetworks.org/projects/nia_ngt0244/
11. Draft best practice guidelines for small scale fracture toughness testing in hydrogen gas of carbon steel pipeline materials. Rev. 4a – 20th June 2024 European Pipeline Research Group https://www.eprg.net
12. Wood Vintage X60 Fracture Toughness in H2, 2024, Project 10486703, Doc 2203695
13. Susceptibility of Vintage Pipe to Embrittlement in Hydrogen-Natural Gas Blends, Liu Cao, Feng Gui, AMPP Annual Conference + Expo 2025, Music City Center, 201 5th Ave S Nashville, TN 37203,United States
14. ASME B31.12-2019, Hydrogen Piping and Pipelines
15. H2PIPE JIP – Transportation of hydrogen gas in offshore pipelines: https://www.dnv.com/article/transportation-of-hydrogen-gas-in-offshore-pipelines-h2pipe-213006/
16. National Gas Services, Data Book [redacted]
17. BS 7910, Guide to methods for assessing the acceptability of flaws in metallic structures
18. Technical Basis for Master Curve for Fatigue Crack Growth of Ferritic Steels in High-Pressure Gaseous Hydrogen in ASME Section VIII-3 Code, ASME 2019 Pressure Vessels & Piping Conference, PVP2019-93907, C San Marchi, J Ronevich.
19. Characteristics of Hydrogen and Natural Gas Blends in the NTS: Work Package 2 – 809337-00-PR-REP-0002 – 18/03/2024

20. DNV-RP-F108, Assessment of flaws in pipeline and riser girth welds, September 2021
21. Crackwise Version 6.3, TWI, Granta Park, Great Abington Cambridge, CB21 6A
22. C. W. San Marchi and J.A. Ronevich "Fatigue and fracture of pipeline steels in high-pressure hydrogen gas", Proceedings of the ASME 2022 Pressure Vessels and Piping Conference PVP2022, July 17-22, 2022, Las Vegas, Nevada, USA.
23. J.A. Ronevich, M. Aghani and C.W. San Marchi "Consistency of fatigue crack growth behaviour of pipeline and low-alloy pressure vessel steels in gaseous hydrogen", International Journal of Hydrogen Energy, 2025, Vol. 136, pp. 686-694
24. B. Bezensek, O. J. Huising, L. Bacchi, P. Roovers and E. Bertelli "EPRG full scale fatigue crack growth test on a modern linepipe material in gaseous hydrogen", Proceedings of the ASME 2024 Pressure Vessels and Piping Conference PVP 2024, Bellevue, Washington, 28 July – 02 August, 2024.
25. API 579 / ASME FFS-1, Fitness-For-Service, International Standard, 2021
26. EDF Energy, "R6: Assessment of the integrity of structures containing defects", Revision 4, Gloucester, UK
27. PD 6550 : Part 2, Explanatory supplement to BS 5500:1988, Part 2. Openings and branch connections.
28. F.A. Leckie F. A. and R.K Penny "Stress concentration factors for the stresses at nozzle intersections at pressure vessels", Welding Research Council Bulletin 90, September 1963.
29. K.R Wichman, A.G Hopper and J.L. Mersnon, "Local stresses in spherical and cylindrical shells due to external loading", Welding Research Council Bulletin 107, October 2002 Update of the March 1979 Revision.
30. J. L. Mershon, K. Mokhtarian, G. V. Ranjan, and E. C. Rodabaugh, "Local stresses in cylindrical shells due to external loadings on nozzles, Supplement to WRC Bulletin 107 (Revision I), September 1987.
31. General purpose finite element package Abaqus, SIMULIA, 2025
32. ASME BPVC VIII 3-2023 KD-10 ASME VIII, Rules for Construction of Pressure Vessels Division 3, Alternative Rules for Construction of High Pressure Vessels".
33. ASME BPVC.VIII.2-2025, Rules for Construction of Pressure Vessels Division 2, Alternative Rules
34. NTS Materials Testing to Enable Hydrogen Injection in High Pressure Pipelines, https://smarter.energynetworks.org/
35. Hydrogen pipeline systems, DNV-RP-123, March 2026

[redacted]

National Gas | Business Use

[redacted]

[redacted]